
Neural Network Architecture Beyond Width and Depth

Zuowei Shen

Department of Mathematics
National University of Singapore
matzuows@nus.edu.sg

Haizhao Yang

Department of Mathematics
University of Maryland, College Park
hzyang@umd.edu

Shijun Zhang*

Department of Mathematics
National University of Singapore
zhangshijun@u.nus.edu

Abstract

This paper proposes a new neural network architecture by introducing an additional dimension called height beyond width and depth. Neural network architectures with height, width, and depth as hyperparameters are called three-dimensional architectures. It is shown that neural networks with three-dimensional architectures are significantly more expressive than the ones with two-dimensional architectures (those with only width and depth as hyperparameters), e.g., standard fully connected networks. The new network architecture is constructed recursively via a nested structure, and hence we call a network with the new architecture nested network (NestNet). A NestNet of height s is built with each hidden neuron activated by a NestNet of height $\leq s - 1$. When $s = 1$, a NestNet degenerates to a standard network with a two-dimensional architecture. It is proved by construction that height- s ReLU NestNets with $\mathcal{O}(n)$ parameters can approximate Lipschitz continuous functions on $[0, 1]^d$ with an error $\mathcal{O}(n^{-(s+1)/d})$, while the optimal approximation error of standard ReLU networks with $\mathcal{O}(n)$ parameters is $\mathcal{O}(n^{-2/d})$. Furthermore, such a result is extended to generic continuous functions on $[0, 1]^d$ with the approximation error characterized by the modulus of continuity. Finally, a numerical example is provided to explore the advantages of the super approximation power of ReLU NestNets.

1 Introduction

In this paper, we design a new neural network architecture by introducing one more dimension, called height, in addition to width and depth in the characterization of dimensions of neural networks. We call neural network architectures with height, width, and depth as hyperparameters three-dimensional architectures. We will show that neural networks with three-dimensional architectures improve the approximation power significantly, compared to standard networks with two-dimensional architectures (those with only width and depth as hyperparameters). The approximation power of standard neural networks has been widely studied in recent years. The optimality of the approximation of standard fully-connected Rectified Linear Unit (ReLU) networks (e.g., see [33, 38, 43, 45]) implies limited room for further improvements. This motivates us to design a new neural network architecture by introducing an additional dimension of height beyond width and depth.

*Corresponding author

We will focus on ReLU ($\max\{x, 0\}$) activation function and use it to demonstrate our ideas. Our new network architecture is constructed recursively via a nested structure, and hence we call a neural network with the new architecture nested network (**NestNet**). A NestNet of height s is built with each hidden neuron activated by a NestNet of height $\leq s - 1$. In the case of $s = 1$, a NestNet degenerates to a standard network with a two-dimensional architecture. Let us use an simple example to explain the height of a NestNet. We say a network is activated by $(\varrho_1, \dots, \varrho_r)$ if each hidden neuron of this network is activated by one of $\varrho_1, \dots, \varrho_r$. Here, $\varrho_1, \dots, \varrho_r$ are trainable functions mapping \mathbb{R} to \mathbb{R} . Then a network of height $s \geq 2$ can be regarded as a $(\varrho_1, \dots, \varrho_r)$ -activated network, where $\varrho_1, \dots, \varrho_r$ are (realized by) networks of height $\leq s - 1$. See an example of a network of height 2 in Figure 1. The network therein can be regarded as a (ϱ_1, ϱ_2) -activated network, where ϱ_1 and ϱ_2 are (realized by) networks of height 1 (i.e., standard networks). The number of parameters in the network of Figure 1 is the sum of the numbers of parameters in $\mathcal{L}_0, \mathcal{L}_1, \mathcal{L}_2$ and ϱ_1, ϱ_2 .

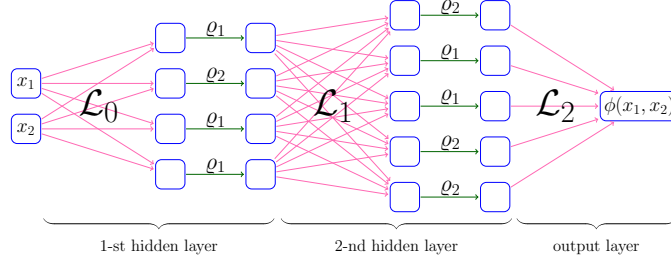


Figure 1: An example of a network of height 2, where ϱ_1 and ϱ_2 are (realized by) networks of height 1 (i.e., standard networks). Here, $\mathcal{L}_0, \mathcal{L}_1$ and \mathcal{L}_2 are affine linear maps.

Remark that a NestNet can be regarded as a sufficiently large standard network by expanding all of its sub-network activation functions. We propose the nested network architecture since it shares the parameters in the sub-network activation functions. This is the key reason why the NestNet has much better approximation property than the standard network. If we regard the network in Figure 1 as a NestNet of height, then the number of parameters is the sum of the numbers of parameters in $\mathcal{L}_0, \mathcal{L}_1, \mathcal{L}_2$ and ϱ_1, ϱ_2 . However, if we expand the network in Figure 1 to a large standard network, then the number of parameters in ϱ_1 and ϱ_2 will be added many times for computing the total number of parameters.

Next, let us discuss our new network architecture from a perspective of hyperparameters. We call the network architecture with only width as a hyperparameter one-dimensional architecture. Its depth and height are both equal to one. Neural networks with this type of architecture are general called shallow networks. See an example in Figure 2(a). We call the network architectures with only width and depth as hyperparameters two-dimensional architecture. Its height is both equal to one. Networks with this type of architecture are general called deep networks. See an example in Figure 2(b). We call the network architectures with height, width, and depth as hyperparameters three-dimensional architecture. This is the architecture introduced in this paper. Networks with this type of architecture are called NestNet. See an example in Figure 2(c). One may refer to Table 1 for the approximation power of networks with these three types of architectures discussed above.

Table 1: Comparison for the approximation error of 1-Lipshitz continuous functions on $[0, 1]^d$ approximated by ReLU NestNets and standard ReLU networks.

	dimension(s)	#parameters	approximation error	remark	reference
one-hidden-layer network	width varies (depth=height=1)	$\mathcal{O}(n)$	n^{-1} for $d = 1$	linear combination	
deep network	width and depth vary (height=1)	$\mathcal{O}(n)$	$n^{-2/d}$	composition	[33, 38, 43, 45]
NestNet of height s	width, depth, and height vary	$\mathcal{O}(n)$	$n^{-(s+1)/d}$	nested composition	this paper

Our main contributions can be summarized as follows. We first propose a three-dimensional neural network architecture by introducing one more dimension called height beyond width and depth. We show that neural networks with three-dimensional architectures are significantly more expressive than the ones with two-dimensional architectures. In particular, we prove by construction that height- s ReLU NestNets with $\mathcal{O}(n)$ parameters can approximate Lipschitz continuous functions on $[0, 1]^d$

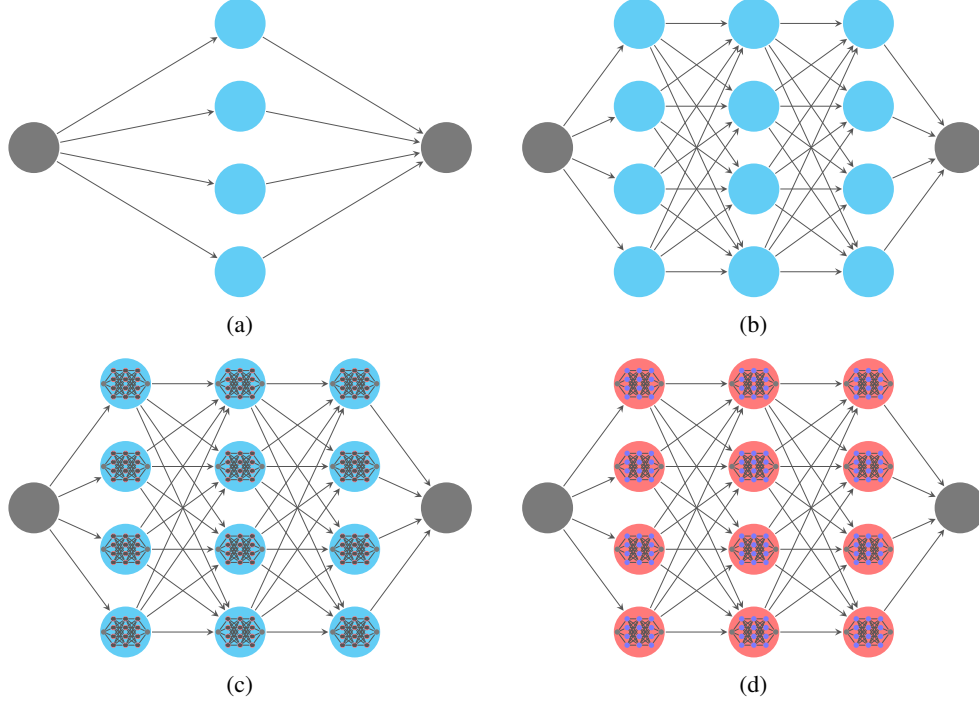


Figure 2: Illustrations of neural networks with one-, two-, and three-dimensional architecture. (a) One-dimensional case (width=4, depth=height=1). (b) Two-dimensional case (width=4, depth=3, height=1). (c) Three-dimensional case (width=4, depth=3, height=3). (d) Zoom-in of an activation function of the network in (c). The network in (d) can also be regarded as a network of height 2.

with an error $\mathcal{O}(n^{-(s+1)/d})$, which is much better than the optimal error $\mathcal{O}(n^{-2/d})$ achieved by standard ReLU networks with $\mathcal{O}(n)$ parameters. In the case of $s+1 \geq d$, the approximation error is bounded by $\mathcal{O}(n^{-(s+1)/d}) \leq \mathcal{O}(n^{-1})$, which means we overcome the curse of dimensionality. Furthermore, we extend our result to generic continuous functions with the approximation error characterized by the modulus of continuity. See Theorem 2.1 and Corollary 2.2 for more details. Finally, we conduct a simple experiment to show the numerical advantages of the super approximation power of ReLU NestNets.

The rest of this paper is organized as follows. In Section 2, we first present our main results and then discuss related work. The proofs of the main results can be found in the appendix. Next, we conduct several experiments to numerically verify our theory in Section 3. Finally, Section 4 concludes this paper with a short discussion.

2 Main results and related work

In this section, we first present our main results and then discuss related work. The proofs of the main results are placed in the appendix.

2.1 Main results

In the rest of this paper, we will use $\mathcal{NN}_s\{n\}$ for $s \in \mathbb{N}^+$ and $n \in \mathbb{N}$ to denote the set of functions realized by height- s ReLU NestNets with as most n parameters. We will present the mathematical definition of $\mathcal{NN}_s\{n\}$. We first discuss some notation regarding affine linear maps. We use \mathcal{L} to denote the set of all affine linear maps, i.e.,

$$\mathcal{L} := \left\{ \mathcal{L} : \mathcal{L}(\mathbf{x}) = \mathbf{W}\mathbf{x} + \mathbf{b}, \mathbf{W} \in \mathbb{R}^{d_2 \times d_1}, \mathbf{b} \in \mathbb{R}^{d_2}, d_1, d_2 \in \mathbb{N}^+ \right\}.$$

Let $\#\mathcal{L}$ denote the number of parameters in $\mathcal{L} \in \mathcal{L}$, i.e.,

$$\#\mathcal{L} = (d_1 + 1)d_2 \quad \text{if } \mathcal{L}(\mathbf{x}) = \mathbf{W}\mathbf{x} + \mathbf{b} \text{ for } \mathbf{W} \in \mathbb{R}^{d_2 \times d_1} \text{ and } \mathbf{b} \in \mathbb{R}^{d_2}.$$

We use $\vec{g} = (\varrho_1, \dots, \varrho_k)$ to denote an activation function vector, where $\varrho_i : \mathbb{R} \rightarrow \mathbb{R}$ is an activation function for each $i \in \{1, \dots, k\}$. When $\vec{g} = (\varrho_1, \dots, \varrho_k)$ is applied to a vector input $\mathbf{x} = (x_1, \dots, x_k)$, we have

$$\vec{g}(\mathbf{x}) = (\varrho_1(x_1), \dots, \varrho_k(x_k)) \quad \text{for any } \mathbf{x} = (x_1, \dots, x_k) \in \mathbb{R}^k.$$

Let $\text{set}(\vec{g})$ denote the function set containing all entries (functions) in \vec{g} . For example, if $\vec{g} = (g_1, g_2, g_3, g_2, g_1)$, then $\text{set}(\vec{g}) = \{g_1, g_2, g_3\}$.

Now we are ready to define $\mathcal{NN}_s\{n\}$ for $n, s \in \mathbb{N}$ recursively in $s \in \mathbb{N}$. In the degenerate case $n = 0$ or $s = 0$, we define

$$\mathcal{NN}_0\{n\} := \{\text{id}_{\mathbb{R}}, \text{ReLU}\} =: \mathcal{NN}_s\{0\} \quad \text{for } n, s \in \mathbb{N},$$

where $\text{id}_{\mathbb{R}} : \mathbb{R} \rightarrow \mathbb{R}$ is the identity map. That is, we regard the identity map and ReLU as height- s ReLU NestNets with 0 parameters or as height-0 ReLU NestNets with n parameters.

Next, let us present the recursive step. For $n, s \in \mathbb{N}^+$, a (vector-valued) function $\phi \in \mathcal{NN}_s\{n\}$ has the following form:

$$\phi = \mathcal{L}_m \circ \vec{g}_m \circ \dots \circ \mathcal{L}_1 \circ \vec{g}_1 \circ \mathcal{L}_0, \quad (1)$$

where $\mathcal{L}_0, \dots, \mathcal{L}_m \in \mathcal{L}$ are affine linear maps. Moreover, Equation (1) shall satisfy the following two conditions:

- Condition on activation functions:

$$\bigcup_{i=1}^m \text{set}(\vec{g}_i) = \{\varrho_1, \dots, \varrho_r\} \quad \text{and} \quad \varrho_j \in \bigcup_{i=0}^{s-1} \mathcal{NN}_i\{n_j\} \quad \text{for } j = 1, \dots, r. \quad (2)$$

Here, \vec{g}_i is an activation function vector for each $i \in \{1, \dots, m\}$. All entries in $\vec{g}_1, \dots, \vec{g}_m$ form an activation function set $\{\varrho_1, \dots, \varrho_r\}$, and ϱ_j for each $j \in \{1, \dots, r\}$ can be realized by a height- i NestNet with $\leq n_j$ parameters for some $i = i_j \leq s-1$. This condition means each hidden neuron is activated by a NestNet of lower height.

- Condition on the number of parameters:

$$\sum_{i=0}^m \#\mathcal{L}_i + \sum_{j=1}^r n_j \leq n. \quad (3)$$

This condition means the total number of parameters is no more than n . The total number of parameters is calculated by adding two parts. The first one is the number of parameters in affine linear maps $\mathcal{L}_0, \dots, \mathcal{L}_m$. The other part is the number of parameters in the activation set $\{\varrho_1, \dots, \varrho_r\}$ formed by the entries in activation function vectors $\vec{g}_1, \dots, \vec{g}_m$.

Then, with two conditions in Equations (2) and (3), we can define $\mathcal{NN}_s\{n\}$ for $n, s \in \mathbb{N}^+$ as follows:

$$\mathcal{NN}_s\{n\} := \left\{ \phi : \phi = \mathcal{L}_m \circ \vec{g}_m \circ \dots \circ \mathcal{L}_1 \circ \vec{g}_1 \circ \mathcal{L}_0, \quad \mathcal{L}_0, \dots, \mathcal{L}_r \in \mathcal{L}, \quad \bigcup_{i=1}^m \text{set}(\vec{g}_i) = \{\varrho_1, \dots, \varrho_r\} \right. \\ \left. \varrho_j \in \bigcup_{i=0}^{s-1} \mathcal{NN}_i\{n_j\} \text{ for } j = 1, \dots, r, \quad \sum_{i=0}^m \#\mathcal{L}_i + \sum_{j=1}^r n_j \leq n \right\}.$$

Remark that, in the definition above, m can be equal to 0. In this case, the function ϕ degenerates to an affine linear map.

In the NestNet example in Figure 1, the function ϕ therein is in $\bigcup_{n \in \mathbb{N}} \mathcal{NN}_2\{n\}$ and the activation function vectors \vec{g}_1 and \vec{g}_2 can be represented as

$$\vec{g}_1 = (\varrho_1, \varrho_2, \varrho_1, \varrho_1) \quad \text{and} \quad \vec{g}_2 = (\varrho_2, \varrho_1, \varrho_1, \varrho_2, \varrho_2).$$

Moreover, the activation function set containing all entries in \vec{g}_1 and \vec{g}_2 is a subset of $\bigcup_{n \in \mathbb{N}} \mathcal{NN}_1\{n\}$, i.e., $\{\varrho_1, \varrho_2\} \subseteq \bigcup_{n \in \mathbb{N}} \mathcal{NN}_1\{n\}$.

Let $C([0, 1]^d)$ denote the set of continuous function on $[0, 1]^d$. By convention, the modulus of continuity of a continuous function $f \in C([0, 1]^d)$ is defined as

$$\omega_f(r) := \sup \{ |f(\mathbf{x}) - f(\mathbf{y})| : \|\mathbf{x} - \mathbf{y}\|_2 \leq r, \mathbf{x}, \mathbf{y} \in [0, 1]^d \} \quad \text{for any } r \geq 0.$$

Under these settings, we can find a function in $\mathcal{NN}_s\{\mathcal{O}(n)\}$ to approximate $f \in C([0, 1]^d)$ with an approximation error $\mathcal{O}(\omega_f(n^{-(s+1)/d}))$, as shown in the main theorem below.

129 **Theorem 2.1.** *Given a continuous function $f \in C([0, 1]^d)$, for any $n, s \in \mathbb{N}^+$ and $p \in [0, \infty]$, there*
 130 *exists $\phi \in \mathcal{NN}_s\{C_{s,d}(n+1)\}$ such that*

$$131 \quad \|\phi(\mathbf{x}) - f(\mathbf{x})\|_{L^p([0,1]^d)} \leq 7\sqrt{d}\omega_f(n^{-(s+1)/d}),$$

132 *where $C_{s,d} = 10^3 d^2 (s+7)^2$ if $p \in [1, \infty)$ and $C_{s,d} = 10^{d+3} d^2 (s+7)^2$ if $p = \infty$.*

133 Remark that the constant $C_{s,d}$ in Theorem 2.1 is valid for all $n \in \mathbb{N}^+$. As we shall see later, $C_{s,d}$ can
 134 be greatly reduced if one only cares about large $n \in \mathbb{N}^+$. Generally, it is challenging to simplify the
 135 approximation error in Theorem 2.1 to make it explicitly depend on n due to the complexity of $\omega_f(\cdot)$.
 136 However, the approximation error can be simplified to an explicit one depending on n in the case of
 137 special target function spaces like Hölder continuous function space. To be exact, if f is a Hölder
 138 continuous function on $[0, 1]^d$ of order $\alpha \in (0, 1]$ with a Hölder constant $\lambda > 0$, then

$$139 \quad |f(\mathbf{x}) - f(\mathbf{y})| \leq \lambda \|\mathbf{x} - \mathbf{y}\|_2^\alpha \quad \text{for any } \mathbf{x}, \mathbf{y} \in [0, 1]^d,$$

140 implying $\omega_f(r) \leq \lambda r^\alpha$ for any $r \geq 0$. This means we can get an exponentially small approximation
 141 error $7\lambda\sqrt{d}n^{-(s+1)\alpha/d}$ as shown in Corollary 2.2 below.

142 **Corollary 2.2.** *Suppose f is a Hölder continuous function on $[0, 1]^d$ of order $\alpha \in (0, 1]$ with a*
 143 *Hölder constant $\lambda > 0$. For any $n, s \in \mathbb{N}^+$ and $p \in [0, \infty]$, there exists $\phi \in \mathcal{NN}_s\{C_{s,d}(n+1)\}$ such*
 144 *that*

$$145 \quad \|\phi(\mathbf{x}) - f(\mathbf{x})\|_{L^p([0,1]^d)} \leq 7\lambda\sqrt{d}n^{-(s+1)\alpha/d},$$

146 *where $C_{s,d} = 10^3 d^2 (s+7)^2$ if $p \in [1, \infty)$ and $C_{s,d} = 10^{d+3} d^2 (s+7)^2$ if $p = \infty$.*

147 In Corollary 2.2, if $\alpha = 1$, i.e., f is a Lipschitz continuous function with a Lipschitz constant
 148 $\lambda > 0$, then the approximation error can be further simplified to $7\lambda\sqrt{d}n^{-(s+1)/d}$. See Table 1 for the
 149 comparison of the approximation error of 1-Lipshitz continuous functions on $[0, 1]^d$ approximated
 150 by ReLU NestNets and standard ReLU networks.

151 2.2 Related work

152 We will connect our results to related existing ones for a deeper understanding. We first compare our
 153 results to existing ones from an approximation perspective. Next, we discuss the connection between
 154 our NestNet architecture and existing trainable activation functions.

155 Discussion from an approximation perspective

156 The study of the approximation power of deep neural networks has become an active topic in recent
 157 years. This topic has been extensively studied from many perspectives, e.g., in terms of combinatorics
 158 [27], topology [7], information theory [29], fat-shattering dimension [1, 21], Vapnik-Chervonenkis
 159 (VC) dimension [6, 14, 31], classical approximation theory [3, 4, 8, 9, 10, 11, 12, 13, 18, 23, 24, 25,
 160 28, 32, 33, 34, 37, 40, 42, 43, 45, 46], etc. To the best of our knowledge, the study of neural network
 161 approximation has two main stages: shallow (one-hidden-layer) networks and deep networks.

162 In the early works of neural network approximation, the approximation power of shallow networks is
 163 investigated. In particular, the universal approximation theorem [11, 17, 18], without approximation
 164 error estimate, showed that a sufficiently large neural network can approximate a target function
 165 in a certain function space arbitrarily well. For one-hidden-layer neural networks of width n and
 166 sufficiently smooth functions, an asymptotic approximation error $\mathcal{O}(n^{-1/2})$ in the L^2 -norm is proved
 167 in [4, 5], leveraging an idea that is similar to Monte Carlo sampling for high-dimensional integrals.

168 Recently, a large number of works focus on the study of deep neural networks. It is shown in
 169 [33, 43, 45] that the optimal approximation error is $\mathcal{O}(n^{-2/d})$ by using ReLU networks with n
 170 parameters to approximate Lipschitz functions on $[0, 1]^d$. This optimal approximation error follows
 171 a natural question: How can we a better approximation error? Generally, there are two ideas to get
 172 better errors. The first one is to consider smaller function spaces, e.g., smooth functions [24, 44] and
 173 band-limited functions [26]. The other one is to introducing new networks, e.g., Floor-ReLU networks
 174 [35], Floor-Exponential-Step (FLES) networks [36], and (Sin, ReLU, 2^x)-activated networks [20].

175 This paper proposes a three-dimensional neural network architecture by introducing one more dimen-
 176 sion called height beyond width and depth. We show that neural networks with three-dimensional

architectures are significantly more expressive than the ones with two-dimensional architectures. To be exact, we prove by construction that height- s ReLU NestNets with $\mathcal{O}(n)$ parameters can approximate Lipschitz continuous functions on $[0, 1]^d$ with an error $\mathcal{O}(n^{-(s+1)/d})$, which is better than the optimal error $\mathcal{O}(n^{-2/d})$ achieved by standard ReLU networks with $\mathcal{O}(n)$ parameters. Such a result can be generalized to generic continuous functions. As shown in Theorem 2.1, the approximation error is $\mathcal{O}(\omega_f(n^{-(s+1)/d}))$ if the target function f is a continuous function on $[0, 1]^d$. Therefore, we overcome the curse of dimensionality if $s + 1 \geq d$ and the variation of $\omega_f(r)$ as $r \rightarrow 0$ is moderate (e.g., $\omega_f(r) \lesssim r^\alpha$ for Hölder continuous functions).

Connection to trainable activation functions

The key idea of trainable activation functions is to add a small number of trainable parameters to existing activation functions. Let us present several existing trainable activation functions as follows. An ReLU-like function is introduced in [15] by modifying the negative part of ReLU using a trainable parameter α , i.e., the Parametric ReLU (PReLU) is defined as

$$\text{PReLU}(x) := \begin{cases} x & \text{if } x \geq 0 \\ \alpha x & \text{if } x < 0. \end{cases}$$

A variant of ELU unit is introduced in [41] by adding two trainable parameters $\beta, \gamma > 0$, i.e., the Parametric ELU (PELU) is given by

$$\text{PELU}(x) := \begin{cases} \frac{\beta}{\gamma} & \text{if } x \geq 0 \\ \beta \left(\exp\left(\frac{x}{\gamma}\right) - 1 \right) x & \text{if } x < 0. \end{cases}$$

Authors in [30] propose a type of Flexible ReLU (FReLU), which is defined via

$$\text{FReLU}(x) := \text{ReLU}(x + \alpha) + \beta,$$

where α and β are two trainable parameters. One may refer to [2] for a survey of modern trainable activation functions. To the best of our knowledge, most existing trainable activation functions can be regarded as **parametric** variants of the original activation functions. That is, they are attained via parameterizing the original activation functions with a small number of (typically 1 or 2) trainable parameters.

By contrast, activation functions in our NestNets are much more flexible. They can be (realized by) either complicated or simple sub-NestNets. That is, we can freely determine the number of parameters in the activation functions of NestNets. In other words, in NestNets, we can randomly distribute the parameters in the affine linear maps and activation functions. In short, compared to the networks with existing trainable activation functions, our NestNets are much flexible and have much more freedom on the choice of activation functions.

3 Experiments

In this section we will conduct a simple experiment to explore the numerical advantages of the super approximation power of ReLU NestNets. To this end, we first discuss the experiment setup in Section 3.1 and then present the experiment results in Section 3.2.

3.1 Experiment setup

We will design a binary classification experiment with sufficiently many data samples. The idea comes from the Archimedean spiral, which can be described by the equation $r = a + b\theta$ in polar coordinates (r, θ) , where a and b are given real numbers. In other words, we will design two sets \mathcal{S}_0 and \mathcal{S}_1 in $[0, 1]^2$ based on the Archimedean spiral, where the label for \mathcal{S}_i is i for $i = 0, 1$.

Let us first define two curves (Archimedean spirals) as follows:

$$\tilde{\mathcal{C}}_i := \left\{ (x, y) : x = r_i \cos \theta, y = r_i \sin \theta, r_i = a_i + b_i \theta, \text{ for } \theta \in [0, s\pi] \right\},$$

for $i = 0, 1$, where $a_0 = 0$, $a_1 = 1$, $b_0 = b_1 = \frac{1}{\pi}$, and $s = 20$. To simplify the discussion below, we normalize $\tilde{\mathcal{C}}_i$ as $\mathcal{C}_i \subseteq [0, 1]^2$, where \mathcal{C}_i is defined by

$$\mathcal{C}_i := \left\{ (x, y) : x = \frac{\tilde{x}}{2(s+2)} + \frac{1}{2}, y = \frac{\tilde{y}}{2(s+2)} + \frac{1}{2}, (\tilde{x}, \tilde{y}) \in \tilde{\mathcal{C}}_i \right\},$$

for $i = 0, 1$. Then, we can define the two desired sets as follows:

$$\mathcal{S}_i := \left\{ (u, v) : \sqrt{(u-x)^2 + (v-y)^2} \leq \varepsilon, (x, y) \in \mathcal{C}_i \right\},$$

for $i = 0, 1$, where $\varepsilon = 0.008$ in our experiments. See an illustration for \mathcal{S}_0 and \mathcal{S}_1 in Figure 3.

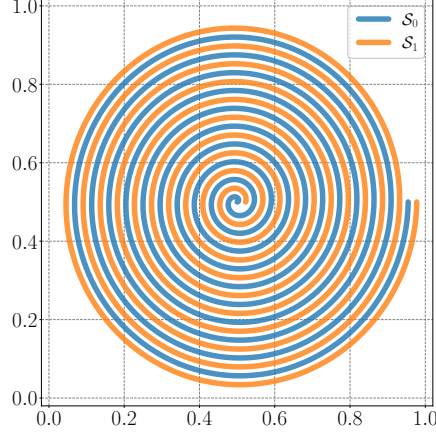


Figure 3: An illustration for \mathcal{S}_0 and \mathcal{S}_1 .

The goal of our experiments is to train a network to approximate the binary classification function f well, where f is defined by

$$f(\mathbf{x}) := \begin{cases} 0 & \text{if } \mathbf{x} \in \mathcal{S}_0 \\ 1 & \text{if } \mathbf{x} \in \mathcal{S}_1. \end{cases}$$

It is easy to verify that \mathcal{S}_0 and \mathcal{S}_1 are closed subsets of $[0, 1]^2$. Then f can be continuously extended to $[0, 1]^2$. Define

$$\tilde{f}(\mathbf{x}) := \frac{\text{dist}(\mathbf{x}, \mathcal{S}_0)}{\text{dist}(\mathbf{x}, \mathcal{S}_0) + \text{dist}(\mathbf{x}, \mathcal{S}_1)} \quad \text{for any } \mathbf{x} \in [0, 1]^2,$$

where

$$\text{dist}(\mathbf{x}, \mathcal{S}_i) := \inf_{\mathbf{y} \in \mathcal{S}_i} \|\mathbf{x} - \mathbf{y}\|_2 \quad \text{for any } \mathbf{x} \in [0, 1]^2 \text{ and } i = 0, 1.$$

It is easy to verify that \tilde{f} is continuous on $[0, 1]^d$ and

$$\tilde{f}(\mathbf{x}) = f(\mathbf{x}) \quad \text{for any } \mathbf{x} \in \mathcal{S}_0 \cup \mathcal{S}_1.$$

That means \tilde{f} is a continuous extension of f . Moreover, the modulus of continuity of the extension \tilde{f} can be easily estimated based on

$$\text{dist}(\mathcal{S}_0, \mathcal{S}_1) := \inf_{\mathbf{x} \in \mathcal{S}_0, \mathbf{y} \in \mathcal{S}_1} \|\mathbf{x} - \mathbf{y}\|_2 > 0.$$

Next, let us discuss the network architecture in our experiments. We consider two type of networks: NestNets and standard networks. We adopt four-hidden-layer fully connected network architecture of width 20, 35, or 50. As for the activation function, we adopt σ for the standard network and ϱ for the NesNet, where σ is ReLU ($\max\{x, 0\}$) and ϱ is realized by a trainable one-hidden-layer ReLU network of width 3. To be exact, ϱ is given by

$$\varrho(x) = \mathbf{w}_1^T \cdot (x\mathbf{w}_0 + \mathbf{b}_0) + b_1 \quad \text{for any } x \in \mathbb{R},$$

where $\mathbf{w}_0, \mathbf{w}_1, \mathbf{b}_0 \in \mathbb{R}^3$ and $b_1 \in \mathbb{R}$ are trainable parameters. There are 10 parameters in ϱ . The initial settings for ϱ in our experiments are $\mathbf{w}_0 = (1, 1, 1)$, $\mathbf{w}_1 = (1, 1, -1)$, $\mathbf{b}_0 = (-0.2, -0.1, 0.0)$, and $b_1 = 0$. See Figure 6 for illustrations. To reduce overfitting and speed up optimization, we take two common regularization methods: dropout [16, 39] and batch normalization [19]. The full architecture is shown in Figure 4.

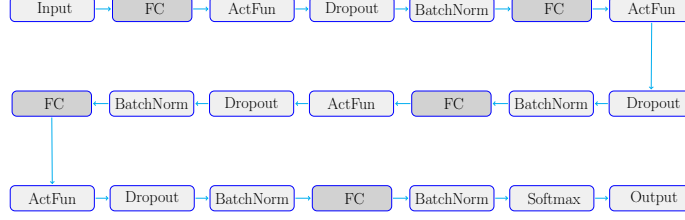


Figure 4: An illustration of the network architecture in the experiments. FC and ActFun are short of fully connected layer and activation function, respectively. ActFun=ReLU (σ) for standard networks; ActFun=sub-network (ϱ) for NestNets.

Finally, we are ready to present our experiment strategy. For each $i \in \{0, 1\}$, we randomly choose 3×10^5 training samples and 3×10^4 test samples in \mathcal{S}_i with label i . Then, we use these 6×10^5 training samples to train our network and use these 6×10^4 test samples to compute the test accuracy. We use the cross-entropy loss function to evaluate the loss between the network and the binary classification function f . The number of epochs and the batch size are set to 80 and 64, respectively. We adopt Adam [22] as the optimization method. For the i -th epoch, the learning rate for the parameters in ϱ is $0.1 \times 0.003 \times 0.85^{i-1}$ and the learning rate for other parameters is $0.003 \times 0.85^{i-1}$. See Tables 2 for more details.

Table 2: Hyperparameters in the experiments.

	standard network	NestNet	
loss function		cross-entropy loss	
number of training samples	6×10^5 in total, with half in \mathcal{S}_i for $i = 0, 1$		
number of test samples	6×10^4 in total, with half in \mathcal{S}_i for $i = 0, 1$		
number of training epochs	80		
training batch size	256		
optimizer	Adam [22]		
learning rate in i -th epoch	$0.003 \times 0.9^{i-1}$	parameters in ϱ	others
		$0.1 \times 0.003 \times 0.9^{i-1}$	$0.003 \times 0.9^{i-1}$

3.2 Experiment results

We will compare the test accuracies for NestNets and standard networks. We adopt the average of largest 20 test accuracies over all 80 epochs as the final test accuracy. As we can see from Table 3 and Figure 5, via adding 10 more parameters (stored in ϱ), NestNets achieve much better test accuracies than standard networks. In an extreme comparison, the test accuracy attained by the NestNet with 1.4×10^3 parameters is still better than that of the standard network with 7.9×10^3 parameters. This numerically verifies that the NestNet has much better approximation power than the standard network.

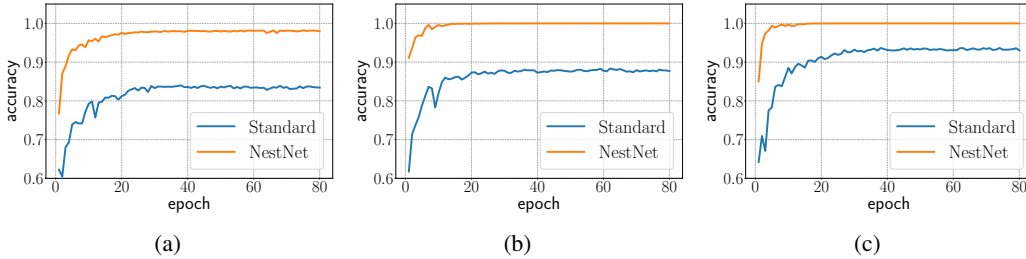


Figure 5: Test accuracy over epochs. (a) Width=20. (b) Width=35. (c) Width=50.

Next, let us discuss the trainable sub-network activation function ϱ . Recall that ϱ is given by

$$\varrho(x) = \mathbf{w}_1^T \cdot (x\mathbf{w}_0 + \mathbf{b}_0) + b_1 \quad \text{for any } x \in \mathbb{R},$$

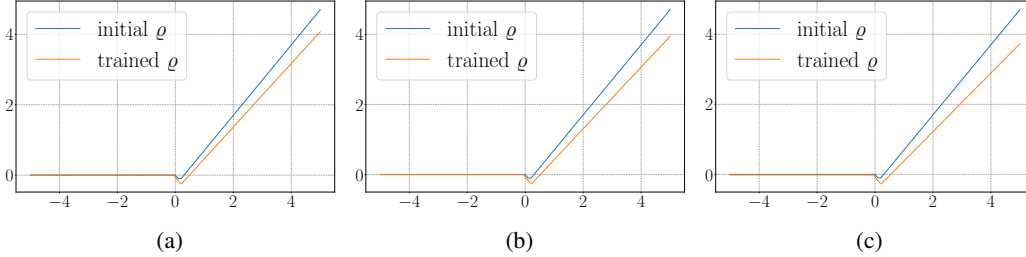
Table 3: Error comparison of standard networks and NestNets.

	width	depth	activation	#parameters	test accuracy
standard network	20	4	ReLU (σ)	1.4×10^3	0.837581
NestNet			sub-network (ϱ)		0.981322
standard network	35	4	ReLU (σ)	4.0×10^3	0.880078
NestNet			sub-network (ϱ)		0.999985
standard network	50	4	ReLU (σ)	7.9×10^3	0.935018
NestNet			sub-network (ϱ)		1.000000

where $w_0, w_1, b_0 \in \mathbb{R}^3$ and $b_1 \in \mathbb{R}$ are trainable parameters. There are 10 parameters in ϱ . We will compare the initial guess and the trained solution for the parameters in ϱ . Our initial settings for ϱ are to make it be a variant of ReLU except for a small neighborhood near 0. As we can see from Table 4, the parameters in ϱ only change a little during the training process. However, the approximation error comparison in Table 3 implies that these little changes of the parameters in ϱ make a big difference. We visualize the difference between the initial ϱ and the trained ϱ in Figure 6.

Table 4: Parameters in ϱ .

	width	w_0	b_0	w_1	b_1
initial		(1, 1, 1)	(-0.2, -0.1, 0.0)	(1, 1, -1)	0
trained	20	(0.9847, 0.9675, 1.0104)	(-0.2223, -0.1620, 0.0607)	(0.9902, 0.9834, -1.0138)	0.0033
	35	(0.9809, 0.9634, 1.0140)	(-0.2265, -0.1675, 0.0667)	(0.9838, 0.9813, -1.0173)	0.0020
	50	(0.9743, 0.9594, 1.0222)	(-0.2303, -0.1634, 0.0535)	(0.9758, 0.9726, -1.0239)	-0.0154

Figure 6: Illustrations of initial ϱ and trained ϱ . (a) Width=20. (b) Width=35. (c) Width=50.

We use a simple example above to show the numerical advantages of the super approximation power of NestNets, which is regarded as a proof of possibility. It would be of great interest to further explore the numerical performance of NestNets to bridge our theoretical result to applications. We believe that NestNets can be further developed and applied to real-world applications.

4 Conclusion

This paper proposes a three-dimensional neural network architecture by introducing one more dimension called height beyond width and depth. We show that neural networks with three-dimensional architectures are significantly more expressive than the ones with two-dimensional architectures. In particular, we prove by construction that height- s ReLU NestNets with $\mathcal{O}(n)$ parameters can approximate Lipschitz continuous functions on $[0, 1]^d$ with an error $\mathcal{O}(n^{-(s+1)/d})$, which is much better than the optimal error $\mathcal{O}(n^{-2/d})$ achieved by standard ReLU networks with $\mathcal{O}(n)$ parameters. Furthermore, we extend our result to generic continuous functions. Finally, we conduct a simple experiment to show the numerical advantages of the super approximation power of ReLU NestNets.

We would like to remark that our analysis was limited on the ReLU activation function and the (Hölder) continuous function space. It would be interesting to extend our conclusions to other activation functions (e.g., tanh and sigmoid functions) and other function spaces (e.g., Lebesgue and

287 Sobolev spaces). Besides, it would be interesting to explore the numerical performance of NestNets
 288 and apply it to real-world applications.

289 Acknowledgments

290 Z. Shen is supported by Tan Chin Tuan Centennial Professorship. H. Yang was partially supported by
 291 the US National Science Foundation under award DMS-1945029.

292 References

- 293 [1] Martin Anthony and Peter L. Bartlett. *Neural Network Learning: Theoretical Foundations*. Cambridge
 294 University Press, New York, NY, USA, 1st edition, 2009.
- 295 [2] Andrea Apicella, Francesco Donnarumma, Francesco Isgrò, and Roberto Prevete. A survey on modern
 296 trainable activation functions. *Neural Networks*, 138:14–32, 2021.
- 297 [3] Chenglong Bao, Qianxiao Li, Zuwei Shen, Cheng Tai, Lei Wu, and Xueshuang Xiang. Approximation
 298 analysis of convolutional neural networks. *Semantic Scholar e-Preprint*, page Corpus ID: 204762668,
 299 2019.
- 300 [4] Andrew R. Barron. Universal approximation bounds for superpositions of a sigmoidal function. *IEEE*
 301 *Transactions on Information Theory*, 39(3):930–945, May 1993.
- 302 [5] Andrew R. Barron and Jason M. Klusowski. Approximation and Estimation for High-Dimensional Deep
 303 Learning Networks, September 2018.
- 304 [6] Peter Bartlett, Vitaly Maiorov, and Ron Meir. Almost linear VC-dimension bounds for piecewise polyno-
 305 mial networks. *Neural Computation*, 10(8):2159–2173, 1998.
- 306 [7] Monica Bianchini and Franco Scarselli. On the complexity of neural network classifiers: A comparison
 307 between shallow and deep architectures. *IEEE Transactions on Neural Networks and Learning Systems*,
 308 25(8):1553–1565, Aug 2014.
- 309 [8] Helmut. Bölcskei, Philipp. Grohs, Gitta. Kutyniok, and Philipp. Petersen. Optimal approximation with
 310 sparsely connected deep neural networks. *SIAM Journal on Mathematics of Data Science*, 1(1):8–45, 2019.
- 311 [9] Minshuo Chen, Haoming Jiang, Wenjing Liao, and Tuo Zhao. Efficient approximation of deep relu
 312 networks for functions on low dimensional manifolds. In H. Wallach, H. Larochelle, A. Beygelzimer,
 313 F. d’Alché-Buc, E. Fox, and R. Garnett, editors, *Advances in Neural Information Processing Systems*,
 314 volume 32. Curran Associates, Inc., 2019.
- 315 [10] Charles K. Chui, Shao-Bo Lin, and Ding-Xuan Zhou. Construction of neural networks for realization of
 316 localized deep learning. *Frontiers in Applied Mathematics and Statistics*, 4:14, 2018.
- 317 [11] George Cybenko. Approximation by superpositions of a sigmoidal function. *MCSS*, 2:303–314, 1989.
- 318 [12] Rémi Gribonval, Gitta Kutyniok, Morten Nielsen, and Felix Voigtlaender. Approximation spaces of deep
 319 neural networks. *arXiv e-prints*, page arXiv:1905.01208, May 2019.
- 320 [13] Ingo Gühring, Gitta Kutyniok, and Philipp Petersen. Error bounds for approximations with deep ReLU
 321 neural networks in $W^{s,p}$ norms. *arXiv e-prints*, page arXiv:1902.07896, Feb 2019.
- 322 [14] Nick Harvey, Christopher Liaw, and Abbas Mehrabian. Nearly-tight VC-dimension bounds for piecewise
 323 linear neural networks. In Satyen Kale and Ohad Shamir, editors, *Proceedings of the 2017 Conference on*
 324 *Learning Theory*, volume 65 of *Proceedings of Machine Learning Research*, pages 1064–1068, Amsterdam,
 325 Netherlands, 07–10 Jul 2017. PMLR.
- 326 [15] Kaiming He, Xiangyu Zhang, Shaoqing Ren, and Jian Sun. Delving deep into rectifiers: Surpassing
 327 human-level performance on imagenet classification. In *2015 IEEE International Conference on Computer*
 328 *Vision (ICCV)*, pages 1026–1034, 2015.
- 329 [16] Geoffrey E. Hinton, Nitish Srivastava, Alex Krizhevsky, Ilya Sutskever, and Ruslan Salakhutdinov. Im-
 330 proving neural networks by preventing co-adaptation of feature detectors. *CoRR*, abs/1207.0580, 2012.
- 331 [17] Kurt Hornik. Approximation capabilities of multilayer feedforward networks. *Neural Networks*, 4(2):251–
 332 257, 1991.

- [18] Kurt Hornik, Maxwell Stinchcombe, and Halbert White. Multilayer feedforward networks are universal approximators. *Neural Networks*, 2(5):359–366, 1989.
- [19] Sergey Ioffe and Christian Szegedy. Batch normalization: Accelerating deep network training by reducing internal covariate shift. In *Proceedings of the 32nd International Conference on International Conference on Machine Learning - Volume 37*, ICML’15, page 448–456. JMLR.org, 2015.
- [20] Yuling Jiao, Yanming Lai, Xiliang Lu, Fengru Wang, Jerry Zhijian Yang, and Yuanyuan Yang. Deep neural networks with ReLU-Sine-Exponential activations break curse of dimensionality on hölder class. *arXiv e-prints*, page arXiv:2103.00542, February 2021.
- [21] Michael J. Kearns and Robert E. Schapire. Efficient distribution-free learning of probabilistic concepts. *J. Comput. Syst. Sci.*, 48(3):464–497, June 1994.
- [22] Diederik P. Kingma and Jimmy Ba. Adam: A method for stochastic optimization. In Yoshua Bengio and Yann LeCun, editors, *3rd International Conference on Learning Representations, ICLR 2015, San Diego, CA, USA, May 7-9, 2015, Conference Track Proceedings*, 2015.
- [23] Qianxiao Li, Ting Lin, and Zuowei Shen. Deep learning via dynamical systems: An approximation perspective. *arXiv e-prints*, page arXiv:1912.10382, December 2019.
- [24] Jianfeng Lu, Zuowei Shen, Haizhao Yang, and Shijun Zhang. Deep network approximation for smooth functions. *SIAM Journal on Mathematical Analysis*, 53(5):5465–5506, 2021.
- [25] Hadrien Montanelli and Haizhao Yang. Error bounds for deep ReLU networks using the Kolmogorov-Arnold superposition theorem. *Neural Networks*, 129:1–6, 2020.
- [26] Hadrien Montanelli, Haizhao Yang, and Qiang Du. Deep ReLU networks overcome the curse of dimensionality for bandlimited functions. *Journal of Computational Mathematics*, 2020.
- [27] Guido F Montufar, Razvan Pascanu, Kyunghyun Cho, and Yoshua Bengio. On the number of linear regions of deep neural networks. In Z. Ghahramani, M. Welling, C. Cortes, N. D. Lawrence, and K. Q. Weinberger, editors, *Advances in Neural Information Processing Systems 27*, pages 2924–2932. Curran Associates, Inc., 2014.
- [28] Ryumei Nakada and Masaaki Imaizumi. Adaptive approximation and generalization of deep neural network with intrinsic dimensionality. *Journal of Machine Learning Research*, 21(174):1–38, 2020.
- [29] Philipp Petersen and Felix Voigtlaender. Optimal approximation of piecewise smooth functions using deep ReLU neural networks. *Neural Networks*, 108:296–330, 2018.
- [30] Suo Qiu, Xiangmin Xu, and Bolun Cai. Frelu: Flexible rectified linear units for improving convolutional neural networks. In *2018 24th International Conference on Pattern Recognition (ICPR)*, pages 1223–1228, Los Alamitos, CA, USA, aug 2018. IEEE Computer Society.
- [31] Akito Sakurai. Tight bounds for the VC-dimension of piecewise polynomial networks. In *Advances in Neural Information Processing Systems*, pages 323–329. Neural information processing systems foundation, 1999.
- [32] Zuowei Shen, Haizhao Yang, and Shijun Zhang. Nonlinear approximation via compositions. *Neural Networks*, 119:74–84, 2019.
- [33] Zuowei Shen, Haizhao Yang, and Shijun Zhang. Deep network approximation characterized by number of neurons. *Communications in Computational Physics*, 28(5):1768–1811, 2020.
- [34] Zuowei Shen, Haizhao Yang, and Shijun Zhang. Deep network approximation: Achieving arbitrary accuracy with fixed number of neurons. *arXiv e-prints*, page arXiv:2107.02397, July 2021.
- [35] Zuowei Shen, Haizhao Yang, and Shijun Zhang. Deep network with approximation error being reciprocal of width to power of square root of depth. *Neural Computation*, 33(4):1005–1036, 03 2021.
- [36] Zuowei Shen, Haizhao Yang, and Shijun Zhang. Neural network approximation: Three hidden layers are enough. *Neural Networks*, 141:160–173, 2021.
- [37] Zuowei Shen, Haizhao Yang, and Shijun Zhang. ReLU network approximation in terms of intrinsic parameters. *arXiv e-prints*, page arXiv:2111.07964, November 2021.
- [38] Zuowei Shen, Haizhao Yang, and Shijun Zhang. Optimal approximation rate of ReLU networks in terms of width and depth. *Journal de Mathématiques Pures et Appliquées*, 157:101–135, 2022.

- 382 [39] Nitish Srivastava, Geoffrey Hinton, Alex Krizhevsky, Ilya Sutskever, and Ruslan Salakhutdinov. Dropout:
383 A simple way to prevent neural networks from overfitting. *Journal of Machine Learning Research*,
384 15(56):1929–1958, 2014.
- 385 [40] Taiji Suzuki. Adaptivity of deep ReLU network for learning in Besov and mixed smooth Besov spaces:
386 optimal rate and curse of dimensionality. In *International Conference on Learning Representations*, 2019.
- 387 [41] Ludovic Trottier, Philippe Giguère, and Brahim Chaib-draa. Parametric exponential linear unit for deep
388 convolutional neural networks. *2017 16th IEEE International Conference on Machine Learning and*
389 *Applications (ICMLA)*, pages 207–214, 2017.
- 390 [42] Dmitry Yarotsky. Error bounds for approximations with deep ReLU networks. *Neural Networks*, 94:103–
391 114, 2017.
- 392 [43] Dmitry Yarotsky. Optimal approximation of continuous functions by very deep ReLU networks. In
393 Sébastien Bubeck, Vianney Perchet, and Philippe Rigollet, editors, *Proceedings of the 31st Conference*
394 *On Learning Theory*, volume 75 of *Proceedings of Machine Learning Research*, pages 639–649. PMLR,
395 06–09 Jul 2018.
- 396 [44] Dmitry Yarotsky and Anton Zhevnerchuk. The phase diagram of approximation rates for deep neural
397 networks. In H. Larochelle, M. Ranzato, R. Hadsell, M. F. Balcan, and H. Lin, editors, *Advances in Neural*
398 *Information Processing Systems*, volume 33, pages 13005–13015. Curran Associates, Inc., 2020.
- 399 [45] Shijun Zhang. Deep neural network approximation via function compositions. *PhD Thesis, National*
400 *University of Singapore*, 2020. URL: <https://scholarbank.nus.edu.sg/handle/10635/186064>.
- 401 [46] Ding-Xuan Zhou. Universality of deep convolutional neural networks. *Applied and Computational*
402 *Harmonic Analysis*, 48(2):787–794, 2020.

403	Contents of main article and appendix	
404	1 Introduction	1
405	2 Main results and related work	3
406	2.1 Main results	3
407	2.2 Related work	5
408	3 Experiments	6
409	3.1 Experiment setup	6
410	3.2 Experiment results	8
411	4 Conclusion	9
412	A Proof of main theorem	14
413	A.1 Notation	14
414	A.2 Detailed proof of Theorem 2.1	15
415	B Proof of auxiliary theorem	17
416	B.1 Key ideas of proving Theorem A.1	17
417	B.2 Detailed proof of Theorem A.1	18
418	C Proof of Proposition B.1	23
419	C.1 Lemmas for proving Proposition B.1	23
420	C.2 Detailed proof of Proposition B.1	26
421	D Proof of Proposition B.2	27
422	D.1 Lemmas for proving Proposition B.2	27
423	D.2 Detailed proof of Proposition B.2	29
424	D.3 Proof of Lemma D.2 for Proposition B.2	31
425	D.3.1 Proof of Lemma D.4 for Lemma D.2	32
426	D.3.2 Proof of Lemma D.5 for Lemma D.2	34

427 A Proof of main theorem

428 In this section, we will prove the main theorem, Theorem 2.1, based on an auxiliary theorem,
 429 Theorem A.1, which will be proved in Section B. Notation throughout this paper are summarized in
 430 Section A.1.

431 A.1 Notation

432 Let us summarize all basic notation used in this paper as follows.

- 433 • Let \mathbb{R} , \mathbb{Q} , and \mathbb{Z} denote the set of real numbers, rational numbers, and integers, respectively.
- 434 • Let \mathbb{N} and \mathbb{N}^+ denote the set of natural numbers and positive natural numbers, respectively.
 435 That is, $\mathbb{N}^+ = \{1, 2, 3, \dots\}$ and $\mathbb{N} = \mathbb{N}^+ \cup \{0\}$.
- 436 • For any $x \in \mathbb{R}$, let $\lfloor x \rfloor := \max\{n : n \leq x, n \in \mathbb{Z}\}$ and $\lceil x \rceil := \min\{n : n \geq x, n \in \mathbb{Z}\}$.
- 437 • Let $\mathbb{1}_S$ be the indicator (characteristic) function of a set S , i.e., $\mathbb{1}_S$ is equal to 1 on S and 0
 438 outside S .
- 439 • The set difference of two sets A and B is denoted by $A \setminus B := \{x : x \in A, x \notin B\}$.
- 440 • Matrices are denoted by bold uppercase letters. For instance, $\mathbf{A} \in \mathbb{R}^{m \times n}$ is a real matrix
 441 of size $m \times n$, and \mathbf{A}^T denotes the transpose of \mathbf{A} . Vectors are denoted as bold lowercase
 442 letters. For example, $\mathbf{v} = [v_1, \dots, v_d]^T = \begin{bmatrix} v_1 \\ \vdots \\ v_d \end{bmatrix} \in \mathbb{R}^d$ is a column vector. Besides, “[” and
 443 “]” are used to partition matrices (vectors) into blocks, e.g., $\mathbf{A} = \begin{bmatrix} \mathbf{A}_{11} & \mathbf{A}_{12} \\ \mathbf{A}_{21} & \mathbf{A}_{22} \end{bmatrix}$.
- 444 • For any $p \in [1, \infty)$, the p -norm (or ℓ^p -norm) of a vector $\mathbf{x} = [x_1, x_2, \dots, x_d]^T \in \mathbb{R}^d$ is defined
 445 by

$$\|\mathbf{x}\|_p = \|\mathbf{x}\|_{\ell^p} := (|x_1|^p + |x_2|^p + \dots + |x_d|^p)^{1/p}.$$

447 In the case $p = \infty$,

$$\|\mathbf{x}\|_\infty = \|\mathbf{x}\|_{\ell^\infty} := \max\{|x_i| : i = 1, 2, \dots, d\}.$$

- 449 • By convention, $\sum_{j=n_1}^{n_2} a_j = 0$ if $n_1 > n_2$, no matter what a_j is for each j .
- 450 • Given any $K \in \mathbb{N}^+$ and $\delta \in (0, \frac{1}{K})$, define a trifling region $\Omega([0, 1]^d, K, \delta)$ of $[0, 1]^d$ as

$$\Omega([0, 1]^d, K, \delta) := \bigcup_{j=1}^d \left\{ \mathbf{x} = [x_1, x_2, \dots, x_d]^T \in [0, 1]^d : x_j \in \bigcup_{k=1}^{K-1} \left(\frac{k}{K} - \delta, \frac{k}{K} \right) \right\}. \quad (4)$$

452 In particular, $\Omega([0, 1]^d, K, \delta) = \emptyset$ if $K = 1$. See Figure 7 for two examples of trifling
 453 regions.

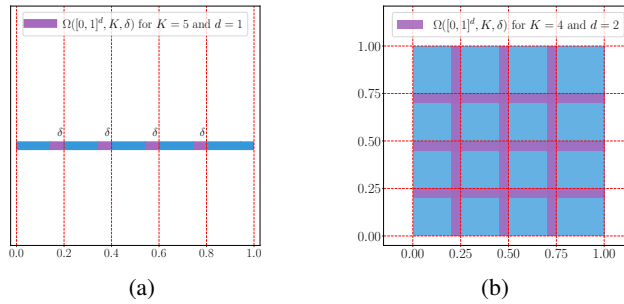


Figure 7: Two examples of trifling regions. (a) $K = 5, d = 1$. (b) $K = 4, d = 2$.

- 454 • For a continuous piecewise linear function $f(x)$, the x values where the slope changes are
 455 typically called **breakpoints**.

- 456 • Let $\sigma : \mathbb{R} \rightarrow \mathbb{R}$ denote the rectified linear unit (ReLU), i.e. $\sigma(x) = \max\{0, x\}$. With
 457 a slight abuse of notation, we define $\sigma : \mathbb{R}^d \rightarrow \mathbb{R}^d$ as $\sigma(\mathbf{x}) = \begin{bmatrix} \max\{0, x_1\} \\ \vdots \\ \max\{0, x_d\} \end{bmatrix}$ for any
 458 $\mathbf{x} = [x_1, \dots, x_d]^T \in \mathbb{R}^d$.
 459 • Let $\mathcal{NN}_s\{n\}$ for $n, s \in \mathbb{N}^+$ denote the set of functions computed by height- s ReLU NestNets
 460 with as most n parameters.
 461 • A function ϕ realized by a ReLU network can be briefly described as follows:
 462
$$\mathbf{x} = \tilde{\mathbf{h}}_0 \xrightarrow[\mathcal{L}_0]{\mathbf{W}_0, \mathbf{b}_0} \mathbf{h}_1 \xrightarrow{\sigma} \tilde{\mathbf{h}}_1 \dots \xrightarrow[\mathcal{L}_{L-1}]{\mathbf{W}_{L-1}, \mathbf{b}_{L-1}} \mathbf{h}_L \xrightarrow{\sigma} \tilde{\mathbf{h}}_L \xrightarrow[\mathcal{L}_L]{\mathbf{W}_L, \mathbf{b}_L} \mathbf{h}_{L+1} = \phi(\mathbf{x}),$$

 463 where $\mathbf{W}_i \in \mathbb{R}^{N_{i+1} \times N_i}$ and $\mathbf{b}_i \in \mathbb{R}^{N_{i+1}}$ are the weight matrix and the bias vector in the i -th
 464 affine linear transformation \mathcal{L}_i , respectively, i.e.,
 465
$$\mathbf{h}_{i+1} = \mathbf{W}_i \cdot \tilde{\mathbf{h}}_i + \mathbf{b}_i =: \mathcal{L}_i(\tilde{\mathbf{h}}_i) \quad \text{for } i = 0, 1, \dots, L,$$

 466 and
 467
$$\tilde{\mathbf{h}}_i = \sigma(\mathbf{h}_i) \quad \text{for } i = 1, 2, \dots, L.$$

 468 In particular, ϕ can be represented in a form of function compositions as follows.
 469
$$\phi = \mathcal{L}_L \circ \sigma \circ \mathcal{L}_{L-1} \circ \sigma \circ \dots \circ \sigma \circ \mathcal{L}_1 \circ \sigma \circ \mathcal{L}_0,$$

which has been illustrated in Figure 8.

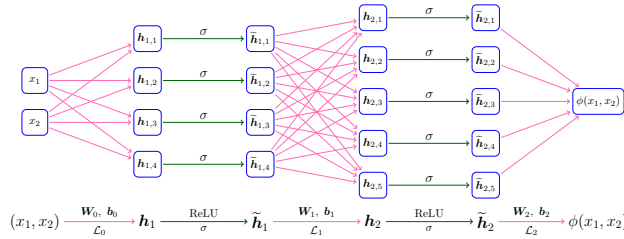


Figure 8: An example of a ReLU network of width 5 and depth 2.

- 470 • The expression “a network of width N and depth L ” means
 471 – The number of neurons in each **hidden** layer of this network (architecture) is no more
 472 than N .
 473 – The number of **hidden** layers of this network (architecture) is no more than L .
 474

475 A.2 Detailed proof of Theorem 2.1

476 The key point of proving Theorem 2.1 is to construct a piecewise constant function to approximate
 477 the target continuous function. However, ReLU NestNets are unable to approximate piecewise
 478 constant functions well the continuity of ReLU NestNets. Thus, we introduce the trifling region
 479 $\Omega([0, 1]^d, K, \delta)$, defined in Equation (4), and use ReLU NestNets to implement piecewise constant
 480 functions outside the trifling region. To simplify the proof of Theorem 2.1, we introduce an auxiliary
 481 theorem, Theorem A.1 below. It can be regarded as a weaker variant of Theorem 2.1, ignoring the
 482 approximation in the trifling region.

483 **Theorem A.1.** *Given a continuous function $f \in C([0, 1]^d)$, for any $n, s \in \mathbb{N}^+$, there exists $\phi \in$
 484 $\mathcal{NN}_s\{355d^2(s+7)^2(2n+1)\}$ such that $\|\phi\|_{L^\infty(\mathbb{R}^d)} \leq |f(\mathbf{0})| + \omega_f(\sqrt{d})$ and*

$$485 |\phi(\mathbf{x}) - f(\mathbf{x})| \leq 6\sqrt{d}\omega_f(n^{-(s+1)/d}) \quad \text{for any } \mathbf{x} \in [0, 1]^d \setminus \Omega([0, 1]^d, K, \delta),$$

486 where $K = \lfloor n^{(s+1)/d} \rfloor$ and δ is an arbitrary number in $(0, \frac{1}{3K}]$.

487 The proof of Theorem A.1 can be found in Section B. By assuming Theorem A.1, we can easily
 488 prove Theorem 2.1 for the case $p \in [1, \infty)$. To prove Theorem 2.1 for the case $p = \infty$, we need to
 489 control the approximation error in the trifling region. To this intent, we introduce a theorem to handle
 the approximation inside the trifling region.

491 **Theorem A.2** (Lemma 3.11 of [45] or Lemma 3.4 of [36]). Given any $\varepsilon > 0$, $K \in \mathbb{N}^+$, and $\delta \in (0, \frac{1}{3K}]$,
 492 assume $f \in C([0, 1]^d)$ and $g : \mathbb{R}^d \rightarrow \mathbb{R}$ is a general function with

$$493 \quad |g(\mathbf{x}) - f(\mathbf{x})| \leq \varepsilon \quad \text{for any } \mathbf{x} \in [0, 1]^d \setminus \Omega([0, 1]^d, K, \delta).$$

494 Then

$$495 \quad |\phi(\mathbf{x}) - f(\mathbf{x})| \leq \varepsilon + d \cdot \omega_f(\delta) \quad \text{for any } \mathbf{x} \in [0, 1]^d,$$

496 where $\phi := \phi_d$ is defined by induction through $\phi_0 := g$ and

$$497 \quad \phi_{i+1}(\mathbf{x}) := \text{mid}(\phi_i(\mathbf{x} - \delta \mathbf{e}_{i+1}), \phi_i(\mathbf{x}), \phi_i(\mathbf{x} + \delta \mathbf{e}_{i+1})) \quad \text{for } i = 0, 1, \dots, d-1,$$

498 where $\{\mathbf{e}_i\}_{i=1}^d$ is the standard basis in \mathbb{R}^d and $\text{mid}(\cdot, \cdot, \cdot)$ is the function returning the middle value of
 499 three inputs.

500 Now, let we prove Theorem 2.1 by assuming Theorem A.1 is true, the proof of which can be found in
 501 Section B.

502 *Proof of Theorem 2.1.* We may assume f is not a constant function since it is a trivial case. Then
 503 $\omega_f(r) > 0$ for any $r > 0$. Let us first consider the case $p \in [1, \infty)$. Set $K = \lfloor n^{(s+1)/d} \rfloor$ and choose a
 504 sufficiently small $\delta \in (0, \frac{1}{3K}]$ such that

$$\begin{aligned} 505 \quad K d \delta (2|f(\mathbf{0})| + 2\omega_f(\sqrt{d}))^p &= \lfloor n^{(s+1)/d} \rfloor d \delta (2|f(\mathbf{0})| + 2\omega_f(\sqrt{d}))^p \\ &\leq (\omega_f(n^{-(s+1)/d}))^p. \end{aligned}$$

506 By Theorem A.1, there exists

$$\begin{aligned} 507 \quad \phi &\in \mathcal{NN}_s\{355d^2(s+7)^2(2n+1)\} \subseteq \mathcal{NN}_s\{355d^2(s+7)^2 \cdot 2(n+1)\} \\ &\subseteq \mathcal{NN}_s\{10^3 d^2(s+7)^2(n+1)\} \end{aligned}$$

508 such that $\|\phi\|_{L^\infty(\mathbb{R}^d)} \leq |f(\mathbf{0})| + \omega_f(\sqrt{d})$ and

$$509 \quad |\phi(\mathbf{x}) - f(\mathbf{x})| \leq 6\sqrt{d}\omega_f(n^{-(s+1)/d}) \quad \text{for any } \mathbf{x} \in [0, 1]^d \setminus \Omega([0, 1]^d, K, \delta).$$

510 Since $\|f\|_{L^\infty([0, 1]^d)} \leq |f(\mathbf{0})| + \omega_f(\sqrt{d})$ and the measure of $\Omega([0, 1]^d, K, \delta)$ is bounded by $K d \delta$, we
 511 have

$$\begin{aligned} 512 \quad \|\phi - f\|_{L^p([0, 1]^d)}^p &= \int_{\Omega([0, 1]^d, K, \delta)} |\phi(\mathbf{x}) - f(\mathbf{x})|^p d\mathbf{x} + \int_{[0, 1]^d \setminus \Omega([0, 1]^d, K, \delta)} |\phi(\mathbf{x}) - f(\mathbf{x})|^p d\mathbf{x} \\ &\leq K d \delta (2|f(\mathbf{0})| + 2\omega_f(\sqrt{d}))^p + (6\sqrt{d}\omega_f(n^{-(s+1)/d}))^p \\ &\leq (\omega_f(n^{-(s+1)/d}))^p + (6\sqrt{d}\omega_f(n^{-(s+1)/d}))^p \leq (7\sqrt{d}\omega_f(n^{-(s+1)/d}))^p. \end{aligned}$$

513 Hence, we have $\|f - \phi\|_{L^p([0, 1]^d)} \leq 7\sqrt{d}\omega_f(n^{-(s+1)/d})$.

514 Next, let us discuss the case $p = \infty$. Set $K = \lfloor n^{(s+1)/d} \rfloor$ and choose a sufficiently small $\delta \in (0, \frac{1}{3K}]$
 515 such that

$$516 \quad d \cdot \omega_f(\delta) \leq \omega_f(n^{-(s+1)/d}).$$

517 By Theorem A.1,

$$518 \quad \phi_0 \in \mathcal{NN}_s\{355d^2(s+7)^2(2n+1)\}$$

519 such that

$$520 \quad |\phi_0(\mathbf{x}) - f(\mathbf{x})| \leq 6\sqrt{d}\omega_f(n^{-(s+1)/d}) \quad \text{for any } \mathbf{x} \in [0, 1]^d \setminus \Omega([0, 1]^d, K, \delta).$$

521 By Theorem A.2 with $g = \phi_0$ and $\varepsilon = 6\sqrt{d}\omega_f(n^{-(s+1)/d})$ therein, we have

$$522 \quad |\phi(\mathbf{x}) - f(\mathbf{x})| \leq \varepsilon + d \cdot \omega_f(\delta) \leq 7\sqrt{d}\omega_f(n^{-(s+1)/d}) \quad \text{for any } \mathbf{x} \in [0, 1]^d,$$

523 where $\phi := \phi_d$ is defined by induction through

$$524 \quad \phi_{i+1}(\mathbf{x}) := \text{mid}(\phi_i(\mathbf{x} - \delta \mathbf{e}_{i+1}), \phi_i(\mathbf{x}), \phi_i(\mathbf{x} + \delta \mathbf{e}_{i+1})) \quad \text{for } i = 0, 1, \dots, d-1,$$

where $\{e_i\}_{i=1}^d$ is the standard basis in \mathbb{R}^d and $\text{mid}(\cdot, \cdot, \cdot)$ is the function returning the middle value of three inputs. It remains to estimate the number of parameters in the NestNet realizing $\phi = \phi_d$. By Lemma 3.1 of [36], $\text{mid}(\cdot, \cdot, \cdot)$ can be realized by a ReLU network of width 14 and depth 2, and hence with at most $14 \times (14 + 1) \times (2 + 1) = 630$ parameters.

By defining a vector-valued function $\Phi_0 : \mathbb{R}^d \rightarrow \mathbb{R}^3$ as

$$\Phi_0(\mathbf{x}) := [\phi_0(\mathbf{x} - \delta \mathbf{e}_1), \phi_0(\mathbf{x}), \phi_0(\mathbf{x} + \delta \mathbf{e}_1)]^T \quad \text{for any } \mathbf{x} \in \mathbb{R}^d,$$

we have $\Phi_0 \in \mathcal{NN}_s\{3^2(355d^2(s+7)^2(2n+1))\}$, implying

$$\begin{aligned} \phi_1 &= \min(\cdot, \cdot, \cdot) \circ \Phi_0 \in \mathcal{NN}_s\left\{630 + 3^2(355d^2(s+7)^2(2n+1))\right\} \\ &\subseteq \mathcal{NN}_s\left\{10(355d^2(s+7)^2(2n+1))\right\}. \end{aligned}$$

Similarly, we have

$$\begin{aligned} \phi &= \phi_d \in \mathcal{NN}_s\left\{10^d(355d^2(s+7)^2(2n+1))\right\} \subseteq \mathcal{NN}_s\left\{10^d(355d^2(s+7)^2 \cdot 2(n+1))\right\} \\ &\subseteq \mathcal{NN}_s\left\{10^{d+3}d^2(s+7)^2(n+1)\right\}. \end{aligned}$$

Thus, we finish the proof of Theorem 2.1.

□

B Proof of auxiliary theorem

We will prove the auxiliary theorem, Theorem A.1, in this section. We first present the key ideas in Section B.1. Next, the detailed proof is presented in Section B.2, based on two propositions in Section B.1, the proofs of which can be found in Sections C and D.

B.1 Key ideas of proving Theorem A.1

Our goal is to construct an almost piecewise constant function realized by a ReLU NestNet to approximate the target function $f \in C([0, 1]^d)$ well. The construction can be divided into three main steps.

1. The first step is the setup. We divide $[0, 1]^d$ into a union of “important” cubes $\{Q_\beta\}_{\beta \in \{0, 1, \dots, K-1\}^d}$ and the trifling region $\Omega([0, 1]^d, K, \delta)$, where $K = \mathcal{O}(n^{(s+1)/d})$ is the number of partitions per dimension. Each Q_β is associated with a representative $\mathbf{x}_\beta \in Q_\beta$ for each vector index β . See Figure 11 for illustrations for $d = 1$ and $d = 2$.

2. Next, we design a vector-valued function $\Phi_1(\mathbf{x})$ to map the whole cube Q_β to its index β for each β . Here, Φ_1 can be defined/constructed via

$$\Phi_1(\mathbf{x}) = [\phi_1(x_1), \phi_1(x_2), \dots, \phi_1(x_d)]^T,$$

where each one-dimensional function ϕ_1 is a step function outside the trifling region, and hence can be realized by a ReLU NestNet.

3. The aim of the final step is essentially to solve a point fitting problem. We will construct a function ϕ_2 realized by a ReLU NestNet to map $\beta \in \{0, 1, \dots, K-1\}^d$ approximately to $f(\mathbf{x}_\beta)$. Then we have

$$\phi_2 \circ \Phi_1(\mathbf{x}) = \phi_2(\beta) \approx f(\mathbf{x}_\beta) \approx f(\mathbf{x}) \quad \text{for any } \mathbf{x} \in Q_\beta \text{ and each } \beta,$$

implying

$$\phi := \phi_2 \circ \Phi_1 \approx f \quad \text{on } [0, 1]^d \setminus \Omega([0, 1]^d, K, \delta).$$

Remark that, in the construction of ϕ_2 , we only need to care about the values of ϕ_2 sampled inside the set $\{0, 1, \dots, K-1\}^d$, which is a key point to ease the design of a ReLU NestNet to realize ϕ_2 as we shall see later.

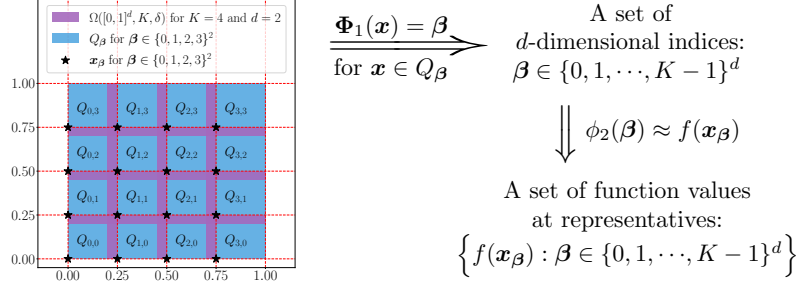


Figure 9: An illustration of the ideas of constructing the desired function $\phi = \phi_2 \circ \Phi_1$. Note that $\phi \approx f$ outside the trifling region since $\phi(x) = \phi_2 \circ \Phi_1(x) = \phi_2(\beta) \approx f(x_{\beta}) \approx f(x)$ for any $x \in Q_{\beta}$ and each $\beta \in \{0, 1, \dots, K-1\}^d$.

Observe that in Figure 9, we have

$$\phi(x) = \phi_2 \circ \Phi_1(x) = \phi_2(\beta) \stackrel{\mathcal{E}_1}{\approx} f(x_{\beta}) \stackrel{\mathcal{E}_2}{\approx} f(x)$$

for any $x \in Q_{\beta}$ and each $\beta \in \{0, 1, \dots, K-1\}^d$. That means $\phi - f$ is controlled by $\mathcal{E}_1 + \mathcal{E}_2$ on $[0, 1]^d \setminus \Omega([0, 1]^d, K, \delta)$. Since $\|x - x_{\beta}\|_2 \leq \sqrt{d}/K$ for any $x \in Q_{\beta}$ and each β , \mathcal{E}_2 is bounded by $\omega_f(\sqrt{d}/K)$. As we shall see later, \mathcal{E}_1 can also be bounded by $\omega_f(\sqrt{d}/K)$ by applying Proposition B.2. Therefore, $\phi - f$ is controlled by $2\omega_f(\sqrt{d}/K)$ outside the trifling region, which deduces the desired approximation error since $K = \mathcal{O}(n^{-(s+1)/d})$.

Finally, we introduce two propositions to simplify the constructions of Φ_1 and ϕ_2 mentioned above. We first show how to construct a ReLU network to implement a one-dimensional step function ϕ_1 in Proposition B.1 below. Then Φ_1 can be defined via

$$\Phi_1(x) := [\phi_1(x_1), \phi_1(x_2), \dots, \phi_1(x_d)]^T \quad \text{for any } x = [x_1, x_2, \dots, x_d]^T \in \mathbb{R}^d.$$

Proposition B.1. *Given any $n, r \in \mathbb{N}^+$, $\delta \in (0, 1)$, and $J \in \mathbb{N}^+$ with $J \leq 2^{n^r}$, there exists $\phi \in \mathcal{NN}_r\{36(r+7)n\}$ such that*

$$\phi(x) = \lfloor x \rfloor \quad \text{for any } x \in \bigcup_{j=0}^{J-1} [j, j+1-\delta]$$

and

$$\phi(x) = J \quad \text{for any } x \in [J, J+1].$$

The construction of ϕ_2 is mainly based on Proposition B.2 below, whose proof relies on the bit extraction technique proposed in [6]. As we shall see later, some pre-processing is necessary for meeting the requirements of applying Proposition B.2 to construct ϕ_2 .

Proposition B.2. *Given any $\varepsilon > 0$ and $n, s \in \mathbb{N}^+$, assume $y_j \geq 0$ for $j = 0, 1, \dots, J-1$ are samples with $J \leq n^{s+1}$ and*

$$|y_j - y_{j-1}| \leq \varepsilon \quad \text{for } j = 1, 2, \dots, J-1.$$

Then there exists $\phi \in \mathcal{NN}_s\{350(s+7)^2(n+1)\}$ such that

$$(i) \quad |\phi(j) - y_j| \leq \varepsilon \text{ for } j = 0, 1, \dots, J-1.$$

$$(ii) \quad 0 \leq \phi(x) \leq \max\{y_j : j = 0, 1, \dots, J-1\} \text{ for any } x \in \mathbb{R}.$$

The proofs of these two propositions can be found in Sections C and D. We will give the detailed proof of Theorem A.1 in Section B.2.

B.2 Detailed proof of Theorem A.1

We essentially construct an almost piecewise constant function realized by a ReLU NestNet with at most $\mathcal{O}(n)$ parameters to approximate f . We may assume f is not a constant function since

593 it is a trivial case. Then $\omega_f(r) > 0$ for any $r > 0$. It is clear that $|f(\mathbf{x}) - f(\mathbf{0})| \leq \omega_f(\sqrt{d})$ for
 594 any $\mathbf{x} \in [0, 1]^d$. By defining $\tilde{f} := f - f(\mathbf{0}) + \omega_f(\sqrt{d})$, we have $\omega_{\tilde{f}}(r) = \omega_f(r)$ for any $r \geq 0$ and
 595 $0 \leq \tilde{f}(\mathbf{x}) \leq 2\omega_f(\sqrt{d})$ for any $\mathbf{x} \in [0, 1]^d$.

596 Set $K = \lfloor n^{(s+1)/d} \rfloor$ and let δ be an arbitrary number in $(0, \frac{1}{3K}]$. The proof can be divided into four
 597 main steps as follows:

- 598 1. Divide $[0, 1]^d$ into a union of sub-cubes $\{Q_\beta\}_{\beta \in \{0, 1, \dots, K-1\}^d}$ and the trifling region
 599 $\Omega([0, 1]^d, K, \delta)$, and denote \mathbf{x}_β as the vertex of Q_β with minimum $\|\cdot\|_1$ norm.
- 600 2. Construct a sub-network based on Proposition B.1 to implement a vector function Φ_1
 601 projecting the whole cube Q_β to the d -dimensional index β for each β , i.e., $\Phi_1(\mathbf{x}) = \beta$ for
 602 all $\mathbf{x} \in Q_\beta$.
- 603 3. Construct a sub-network to implement a function ϕ_2 mapping the index β approximately to
 604 $\tilde{f}(\mathbf{x}_\beta)$. This core step can be further divided into three sub-steps:
 - 605 3.1. Construct a sub-network to implement ψ_1 bijectively mapping the index set
 606 $\{0, 1, \dots, K-1\}^d$ to an auxiliary set $\mathcal{A}_1 \subseteq \{\frac{j}{2K^d} : j = 0, 1, \dots, 2K^d\}$ defined later.
 607 See Figure 12 for an illustration.
 - 608 3.2. Determine a continuous piecewise linear function g with a set of breakpoints $\mathcal{A}_1 \cup$
 609 $\mathcal{A}_2 \cup \{1\}$, where $\mathcal{A}_2 \subseteq \{\frac{j}{2K^d} : j = 0, 1, \dots, 2K^d\}$ is a set defined later. Moreover, g
 610 should satisfy two conditions: 1) the values of g at breakpoints in \mathcal{A}_1 is given based on
 611 $\{\tilde{f}(\mathbf{x}_\beta)\}_\beta$, i.e., $g \circ \psi_1(\beta) = \tilde{f}(\mathbf{x}_\beta)$; 2) the values of g at breakpoints in $\mathcal{A}_2 \cup \{1\}$ is
 612 defined to reduce the variation of g , which is necessary for applying Proposition B.2.
 - 613 3.3. Apply Proposition B.2 to construct a sub-network to implement a function ψ_2 approxi-
 614 mating g well on $\mathcal{A}_1 \cup \mathcal{A}_2 \cup \{1\}$. Then the desired function ϕ_2 is given by $\phi_2 = \psi_2 \circ \psi_1$
 615 satisfying $\phi_2(\beta) = \psi_2 \circ \psi_1(\beta) \approx g \circ \psi_1(\beta) = \tilde{f}(\mathbf{x}_\beta)$.
- 616 4. Construct the final network to implement the desired function ϕ via $\phi = \phi_2 \circ \Phi_1 + f(\mathbf{0}) -$
 617 $\omega_f(\sqrt{d})$. Then we have $\phi_2 \circ \Phi_1(\mathbf{x}) = \phi_2(\beta) \approx \tilde{f}(\mathbf{x}_\beta) \approx \tilde{f}(\mathbf{x})$ for any $\mathbf{x} \in Q_\beta$ and
 618 $\beta \in \{0, 1, \dots, K-1\}^d$, implying $\phi(\mathbf{x}) = \phi_2 \circ \Phi_1(\mathbf{x}) + f(\mathbf{0}) - \omega_f(\sqrt{d}) \approx \tilde{f}(\mathbf{x}) + f(\mathbf{0}) -$
 619 $\omega_f(\sqrt{d}) = f(\mathbf{x})$.

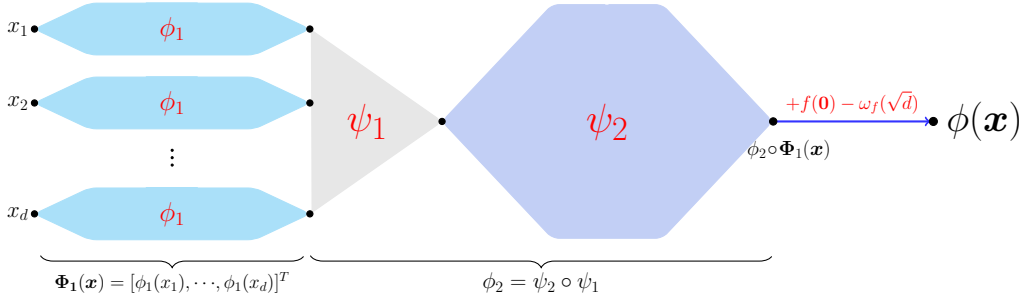


Figure 10: An illustration of the NestNet architecture realizing $\phi = \phi_2 \circ \Phi_1 + f(\mathbf{0}) - \omega_f(\sqrt{d})$. Here, ϕ_1 is implemented via Proposition B.1; $\psi_1 : \mathbb{R}^d \rightarrow \mathbb{R}$ is an affine linear function; ψ_2 is implemented via Proposition B.2, respectively.

620 See Figure 10 for an illustration of the NestNet architecture realizing $\phi = \phi_2 \circ \Phi_1 + f(\mathbf{0}) - \omega_f(\sqrt{d})$.
 621 The details of the steps mentioned above can be found below.

622 **Step 1:** Divide $[0, 1]^d$ into $\{Q_\beta\}_{\beta \in \{0, 1, \dots, K-1\}^d}$ and $\Omega([0, 1]^d, K, \delta)$.

623 Define $\mathbf{x}_\beta := \beta/K$ and

$$624 \quad Q_\beta := \left\{ \mathbf{x} = [x_1, x_2, \dots, x_d]^T \in [0, 1]^d : x_i \in \left[\frac{\beta_i}{K}, \frac{\beta_i+1}{K} - \delta \cdot \mathbf{1}_{\{\beta_i \leq K-2\}} \right], \quad i = 1, 2, \dots, d \right\}$$

625 for each d -dimensional index $\beta = [\beta_1, \beta_2, \dots, \beta_d]^T \in \{0, 1, \dots, K-1\}^d$. Recall that $\Omega([0, 1]^d, K, \delta)$
 626 is the trifling region defined in Equation (4). Apparently, \mathbf{x}_β is the vertex of Q_β with minimum $\|\cdot\|_1$

627 norm and

628
$$[0, 1]^d = \left(\cup_{\beta \in \{0, 1, \dots, K-1\}^d} Q_\beta \right) \cup \Omega([0, 1]^d, K, \delta).$$

629 See Figure 11 for illustrations.

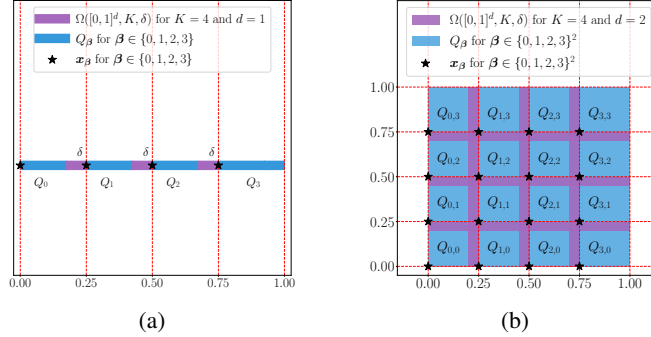


Figure 11: Illustrations of $\Omega([0, 1]^d, K, \delta)$, Q_β , and x_β for $\beta \in \{0, 1, \dots, K-1\}^d$. (a) $K = 4$ and $d = 1$. (b) $K = 4$ and $d = 2$.

630 **Step 2:** Construct Φ_1 mapping $x \in Q_\beta$ to β .

631 Note that

632
$$K-1 = \lfloor n^{(s+1)/d} \rfloor - 1 \leq n^{s+1} \leq (n^s)^2 \leq 4^{(n^s)} = 2^{2(n^s)} \leq 2^{(2n)^s} = 2^{\tilde{n}^s},$$

633 where $\tilde{n} = 2n$. By Proposition B.1 with $r = s$ and $J = K-1 \leq 2^{\tilde{n}^s} = 2^{\tilde{n}^r}$ therein, there exists

634
$$\tilde{\phi}_1 \in \mathcal{NN}_s\{36(s+7)\tilde{n}\} = \mathcal{NN}_s\{36(s+7)(2n)\} = \mathcal{NN}_s\{72(s+7)n\}$$

635 such that

636
$$\tilde{\phi}_1(x) = \lfloor x \rfloor \quad \text{for any } x \in \bigcup_{k=0}^{K-2} [k, k+1-\tilde{\delta}] \text{ with } \tilde{\delta} = K\delta$$

637 and

638
$$\tilde{\phi}_1(x) = K-1 \quad \text{for any } x \in [K-1, K].$$

639 Define $\phi_1(x) := \tilde{\phi}_1(Kx)$ for any $x \in \mathbb{R}$. Then, we have $\phi_1 \in \mathcal{NN}_s\{72(s+7)n\}$ and

640
$$\phi_1(x) = k \quad \text{if } x \in \left[\frac{k}{K}, \frac{k+1}{K} - \delta \cdot \mathbb{1}_{\{k \leq K-2\}} \right] \quad \text{for } k = 0, 1, \dots, K-1.$$

641 It follows that $\phi_1(x_i) = \beta_i$ if $\mathbf{x} = [x_1, x_2, \dots, x_d]^T \in Q_\beta$ for each $\beta = [\beta_1, \beta_2, \dots, \beta_d]^T$.

642 By defining

643
$$\Phi_1(\mathbf{x}) := [\phi_1(x_1), \phi_1(x_2), \dots, \phi_1(x_d)]^T \quad \text{for any } \mathbf{x} = [x_1, x_2, \dots, x_d]^T \in \mathbb{R}^d,$$

644 we have

645
$$\Phi_1(\mathbf{x}) = \beta \quad \text{if } \mathbf{x} \in Q_\beta \quad \text{for each } \beta \in \{0, 1, \dots, K-1\}^d. \quad (5)$$

646 **Step 3:** Construct ϕ_2 mapping β approximately to $\tilde{f}(\mathbf{x}_\beta)$.

647 The construction of the sub-network implementing ϕ_2 is essentially based on Proposition B.2. To
648 meet the requirements of applying Proposition B.2, we first define two auxiliary sets \mathcal{A}_1 and \mathcal{A}_2 as

649
$$\mathcal{A}_1 := \left\{ \frac{i}{K^{d-1}} + \frac{k}{2K^d} : i = 0, 1, \dots, K^{d-1}-1 \quad \text{and} \quad k = 0, 1, \dots, K-1 \right\}$$

650 and

651
$$\mathcal{A}_2 := \left\{ \frac{i}{K^{d-1}} + \frac{K+k}{2K^d} : i = 0, 1, \dots, K^{d-1}-1 \quad \text{and} \quad k = 0, 1, \dots, K-1 \right\}.$$

652 Clearly,

653
$$\mathcal{A}_1 \cup \mathcal{A}_2 \cup \{1\} = \left\{ \frac{j}{2K^d} : j = 0, 1, \dots, 2K^d \right\} \quad \text{and} \quad \mathcal{A}_1 \cap \mathcal{A}_2 = \emptyset.$$

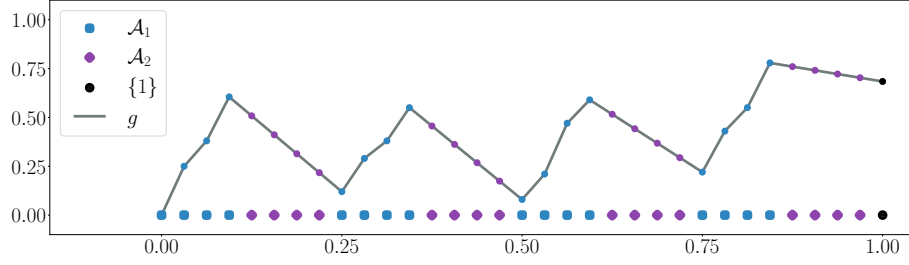


Figure 12: An illustration of \mathcal{A}_1 , \mathcal{A}_2 , $\{1\}$, and g for $K = 4$ and $d = 2$.

See Figure 11 for an illustration of \mathcal{A}_1 and \mathcal{A}_2 . Next, we further divide this step into three sub-steps.

Step 3.1: Construct ψ_1 bijectively mapping $\{0, 1, \dots, K-1\}^d$ to \mathcal{A}_1 .

Inspired by the binary representation, we define

$$\psi_1(\mathbf{x}) := \frac{x_d}{2K^d} + \sum_{i=1}^{d-1} \frac{x_i}{K^i} \quad \text{for any } \mathbf{x} = [x_1, x_2, \dots, x_d]^T \in \mathbb{R}^d. \quad (6)$$

Then ψ_1 is a linear function bijectively mapping the index set $\{0, 1, \dots, K-1\}^d$ to

$$\begin{aligned} \left\{ \psi_1(\beta) : \beta \in \{0, 1, \dots, K-1\}^d \right\} &= \left\{ \frac{\beta_d}{2K^d} + \sum_{i=1}^{d-1} \frac{\beta_i}{K^i} : \beta \in \{0, 1, \dots, K-1\}^d \right\} \\ &= \left\{ \frac{i}{K^{d-1}} + \frac{k}{2K^d} : i = 0, 1, \dots, K^{d-1}-1 \quad \text{and} \quad k = 0, 1, \dots, K-1 \right\} = \mathcal{A}_1. \end{aligned}$$

Step 3.2: Construct g to satisfy $g \circ \psi_1(\beta) = \tilde{f}(\mathbf{x}_\beta)$ and to meet the requirements of applying Proposition B.2.

Let $g : [0, 1] \rightarrow \mathbb{R}$ be a continuous piecewise linear function with a set of breakpoints

$$\left\{ \frac{j}{2K^d} : j = 0, 1, \dots, 2K^d \right\} = \mathcal{A}_1 \cup \mathcal{A}_2 \cup \{1\}.$$

Moreover, the values of g at these breakpoints are assigned as follows:

- At the breakpoint 1, let $g(1) = \tilde{f}(\mathbf{1})$, where $\mathbf{1} = [1, 1, \dots, 1]^T \in \mathbb{R}^d$.

- For the breakpoints in $\mathcal{A}_1 = \left\{ \psi_1(\beta) : \beta \in \{0, 1, \dots, K-1\}^d \right\}$, we set

$$g(\psi_1(\beta)) = \tilde{f}(\mathbf{x}_\beta) \quad \text{for any } \beta \in \{0, 1, \dots, K-1\}^d. \quad (7)$$

- The values of g at the breakpoints in \mathcal{A}_2 are assigned to reduce the variation of g , which is a requirement of applying Proposition B.2. Recall that

$$\left\{ \frac{i}{K^{d-1}} - \frac{K+1}{2K^d}, \frac{i}{K^{d-1}} \right\} \subseteq \mathcal{A}_1 \cup \{1\} \quad \text{for } i = 1, 2, \dots, K^{d-1},$$

implying the values of g at $\frac{i}{K^{d-1}} - \frac{K+1}{2K^d}$ and $\frac{i}{K^{d-1}}$ have been assigned in the previous cases for. Thus, the values of g at the breakpoints in \mathcal{A}_2 can be successfully assigned by letting g linear on each interval $[\frac{i}{K^{d-1}} - \frac{K+1}{2K^d}, \frac{i}{K^{d-1}}]$ for $i = 1, 2, \dots, K^{d-1}$ since $\mathcal{A}_2 \subseteq \bigcup_{i=1}^{K^{d-1}} [\frac{i}{K^{d-1}} - \frac{K+1}{2K^d}, \frac{i}{K^{d-1}}]$. See Figure 12 for an illustration.

Apparently, such a function g exists. See Figure 12 for an illustration of g . It is easy to verify that

$$\left| g\left(\frac{j}{2K^d}\right) - g\left(\frac{j-1}{2K^d}\right) \right| \leq \max \left\{ \omega_{\tilde{f}}\left(\frac{\sqrt{d}}{K}\right), \frac{\omega_{\tilde{f}}(\sqrt{d})}{K} \right\} \leq \omega_{\tilde{f}}\left(\frac{\sqrt{d}}{K}\right) = \omega_f\left(\frac{\sqrt{d}}{K}\right)$$

for $j = 1, 2, \dots, 2K^d$. Moreover, we have

$$0 \leq g\left(\frac{j}{2K^d}\right) \leq 2\omega_f(\sqrt{d}) \quad \text{for } j = 0, 1, \dots, 2K^d.$$

679 **Step 3.3:** Construct ψ_2 approximating g well on $\mathcal{A}_1 \cup \mathcal{A}_2 \cup \{1\}$.

680 Observe that

$$681 \quad 2K^d = 2(\lfloor n^{(s+1)/d} \rfloor)^d \leq 2n^{s+1} \leq (2n)^{s+1} = \tilde{n}^{s+1}, \quad \text{where } \tilde{n} = 2n.$$

682 By Proposition B.2 with $y_j = g(\frac{j}{2K^d})$ and $\varepsilon = \omega_f(\frac{\sqrt{d}}{K}) > 0$ therein, there exists

$$683 \quad \tilde{\psi}_2 \in \mathcal{NN}_s\{350(s+7)^2(\tilde{n}+1)\} = \mathcal{NN}_s\{350(s+7)^2(2n+1)\}$$

684 such that

$$685 \quad |\tilde{\psi}_2(j) - g(\frac{j}{2K^d})| \leq \omega_f(\frac{\sqrt{d}}{K}) \quad \text{for } j = 0, 1, \dots, 2K^d - 1$$

686 and

$$687 \quad 0 \leq \tilde{\psi}_2(x) \leq \max\{g(\frac{j}{2K^d}) : j = 0, 1, \dots, 2K^d - 1\} \leq 2\omega_f(\sqrt{d}) \quad \text{for any } x \in \mathbb{R}.$$

688 By defining $\psi_2(x) := \tilde{\psi}_2(2K^d x)$ for any $x \in \mathbb{R}$, we have

$$689 \quad 0 \leq \psi_2(x) = \tilde{\psi}_2(2K^d x) \leq 2\omega_f(\sqrt{d}) \quad \text{for any } x \in \mathbb{R} \quad (8)$$

690 and

$$691 \quad |\psi_2(\frac{j}{2K^d}) - g(\frac{j}{2K^d})| = |\tilde{\psi}_2(j) - g(\frac{j}{2K^d})| \leq \omega_f(\frac{\sqrt{d}}{K}) \quad \text{for } j = 0, 1, \dots, 2K^d - 1. \quad (9)$$

692 Let us end Step 3 by defining the desired function ϕ_2 as $\phi_2 := \psi_2 \circ \psi_1$. Recall that $\psi_1(\beta) = \mathcal{A}_1 \subseteq$
 693 $\{\frac{j}{2K^d} : j = 0, 1, \dots, 2K^d - 1\}$. Then, by Equations (7) and (9), we have

$$694 \quad |\phi_2(\beta) - \tilde{f}(\mathbf{x}_\beta)| = |\psi_2(\psi_1(\beta)) - g(\psi_1(\beta))| \leq \omega_f(\frac{\sqrt{d}}{K}) \quad (10)$$

695 for any $\beta \in \{0, 1, \dots, K-1\}^d$. Moreover, by Equation (8) and $\phi_2 = \psi_2 \circ \psi_1$, we have

$$696 \quad 0 \leq \phi_2(\mathbf{x}) = \psi_2(\psi(\mathbf{x})) \leq 2\omega_f(\sqrt{d}) \quad \text{for any } \mathbf{x} \in \mathbb{R}^d. \quad (11)$$

697 **Step 4:** Construct the final network to implement the desired function ϕ .

698 Define $\phi := \phi_2 \circ \Phi_1 + f(\mathbf{0}) - \omega_f(\sqrt{d})$. By Equation (11), we have

$$699 \quad 0 \leq \phi_2 \circ \Phi_1(\mathbf{x}) \leq 2\omega_f(\sqrt{d})$$

700 for any $\mathbf{x} \in \mathbb{R}^d$, implying

$$701 \quad f(\mathbf{0}) - \omega_f(\sqrt{d}) \leq \phi(\mathbf{x}) = \phi_2 \circ \Phi_1(\mathbf{x}) + f(\mathbf{0}) - \omega_f(\sqrt{d}) \leq f(\mathbf{0}) + \omega_f(\sqrt{d}).$$

702 It follows that $\|\phi\|_{L^\infty(\mathbb{R}^d)} \leq |f(\mathbf{0})| + \omega_f(\sqrt{d})$.

703 Next, let us estimate the approximation error. Recall that $f = \tilde{f} + f(\mathbf{0}) - \omega_f(\sqrt{d})$ and $\phi = \phi_2 \circ \Phi_1 +$
 704 $f(\mathbf{0}) - \omega_f(\sqrt{d})$. By Equations (5) and (10), for any $\mathbf{x} \in Q_\beta$ and $\beta \in \{0, 1, \dots, K-1\}^d$, we have

$$\begin{aligned} 705 \quad |f(\mathbf{x}) - \phi(\mathbf{x})| &= |\tilde{f}(\mathbf{x}) - \phi_2 \circ \Phi_1(\mathbf{x})| = |\tilde{f}(\mathbf{x}) - \phi_2(\beta)| \\ &\leq |\tilde{f}(\mathbf{x}) - \tilde{f}(\mathbf{x}_\beta)| + |\tilde{f}(\mathbf{x}_\beta) - \phi_2(\beta)| \\ &\leq \omega_f(\frac{\sqrt{d}}{K}) + \omega_f(\frac{\sqrt{d}}{K}) \leq 2\omega_f(2\sqrt{d}n^{-(s+1)/d}), \end{aligned}$$

706 where the last inequality comes from the fact

$$707 \quad K = \lfloor n^{(s+1)/d} \rfloor \geq n^{(s+1)/d}/2 \quad \text{for } n \in \mathbb{N}^+.$$

708 Recall the fact $\omega_f(j \cdot r) \leq j \cdot \omega_f(r)$ for any $j \in \mathbb{N}^+$ and $r \in [0, \infty)$. Therefore, for any $\mathbf{x} \in$
 709 $\bigcup_{\beta \in \{0, 1, \dots, K-1\}^d} Q_\beta = [0, 1]^d \setminus \Omega([0, 1]^d, K, \delta)$, we have

$$\begin{aligned} 710 \quad |\phi(\mathbf{x}) - f(\mathbf{x})| &\leq 2\omega_f(2\sqrt{d}n^{-(s+1)/d}) \leq 2\lceil 2\sqrt{d} \rceil \omega_f(n^{-(s+1)/d}) \\ &\leq 6\sqrt{d}\omega_f(n^{-(s+1)/d}). \end{aligned}$$

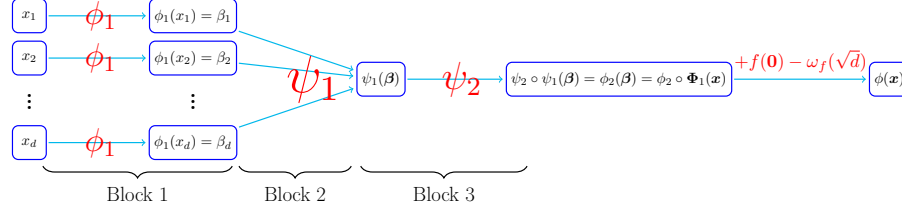


Figure 13: An illustration of the final NestNet realizing $\phi = \phi_2 \circ \Phi_1 + f(\mathbf{0}) - \omega_f(\sqrt{d})$ for $\mathbf{x} = [x_1, x_2, \dots, x_d]^T \in Q_\beta$ for each $\beta \in \{0, 1, \dots, K-1\}^d$.

It remains to estimate the number of parameters in the NestNet realizing ϕ , which is shown in Figure 13. Recall that $\phi_1 \in \mathcal{NN}_s\{72(s+7)n\}$, ψ_1 is an affine linear map, and $\psi_2 \in \mathcal{NN}_s\{350(s+7)^2(2n+1)\}$. Therefore, $\phi = \phi_2 \circ \Phi_1 + f(\mathbf{0}) - \omega_f(\sqrt{d})$ can be realized by a height- s NestNet with at most

$$\underbrace{d^2(72(s+7)n)}_{\text{Block 1}} + \underbrace{(d+1)}_{\text{Block 2}} + \underbrace{350(s+7)^2(2n+1)}_{\text{Block 3}} + 1 \leq 355d^2(s+7)^2(2n+1)$$

parameters, which means we finish the proof of Theorem A.1.

C Proof of Proposition B.1

The key point of proving Proposition B.1 is the composition architecture of neural networks. To simplify the proof, we first establish several lemmas for proving Proposition B.1 in Section C.1. Next, we present the detailed proof of Proposition B.1 in Section C.2 based on the lemmas established in Section C.1.

C.1 Lemmas for proving Proposition B.1

Lemma C.1. *Given any $n, r \in \mathbb{N}^+$ and $\delta \in (0, \frac{1}{C(r,n)})$ with $C(r,n) = \prod_{i=1}^r 2^{n^i}$, there exists $\phi \in \mathcal{NN}_r\{(12r+68)n\}$ such that*

$$\phi(x) = \lfloor x \rfloor \quad \text{for any } x \in \bigcup_{\ell=0}^{2^{n^r}-1} [\ell, \ell+1 - C(r,n) \cdot \delta].$$

We will prove Lemma C.1 by induction. To simplify the proof, we introduce two lemmas for the base case and the induction step.

First, we introduce the following lemma for the base case of proving Lemma C.1.

Lemma C.2. *Given any $n \in \mathbb{N}^+$ and $\delta \in (0, 1)$, then there exists a function ϕ realized by a ReLU network of width 4 and depth $4n-1$ such that*

$$\phi(x) = \lfloor x \rfloor \quad \text{for any } x \in \bigcup_{\ell=0}^{2^n-1} [\ell, \ell+1 - \delta].$$

Proof. Set $\tilde{\delta} = 2^{-n}\delta$ and define

$$\phi_0(x) := \frac{\sigma(x-1+\tilde{\delta}) - \sigma(x-1)}{\tilde{\delta}} \quad \text{for } x \in \mathbb{R}.$$

Clearly, ϕ_0 can be realized by a one-hidden-layer ReLU network of width 2. Moreover, we have

$$\phi_0(x) = \frac{\sigma(x-1+\tilde{\delta}) - \sigma(x-1)}{\tilde{\delta}} = \frac{0-0}{\tilde{\delta}} = 0 \quad \text{if } x \in [0, 1-\tilde{\delta}]$$

and

$$\phi_0(x) = \frac{\sigma(x-1+\tilde{\delta}) - \sigma(x-1)}{\tilde{\delta}} = \frac{(x-1+\tilde{\delta}) - (x-1)}{\tilde{\delta}} = 1 \quad \text{if } x \in [1, 2-\tilde{\delta}].$$

738 By fixing

$$739 \quad x \in \bigcup_{\ell=0}^{2^n-1} [\ell, \ell+1-\delta] = \bigcup_{\ell=0}^{2^n-1} [\ell, \ell+1-2^n\tilde{\delta}],$$

740 we have $\lfloor x \rfloor \in \{0, 1, \dots, 2^n-1\}$, implying that $\lfloor x \rfloor$ can be represented as

$$741 \quad \lfloor x \rfloor = \sum_{i=0}^{n-1} z_i 2^i \quad \text{for } z_0, z_1, \dots, z_{n-1} \in \{0, 1\}.$$

742 Then, for $j = 0, 1, \dots, n-1$, we have $\sum_{i=0}^j z_i 2^i + 1 \leq z_j 2^j + \sum_{i=0}^{j-1} 2^i + 1 \leq z_j 2^j + 2^j$, implying

$$743 \quad \frac{x - \sum_{i=j+1}^{n-1} z_i 2^i}{2^j} \in \left[\frac{\lfloor x \rfloor - \sum_{i=j+1}^{n-1} z_i 2^i}{2^j}, \frac{\lfloor x \rfloor + 1 - 2^n \tilde{\delta} - \sum_{i=j+1}^{n-1} z_i 2^i}{2^j} \right] = \left[\frac{\sum_{i=0}^j z_i 2^i}{2^j}, \frac{\sum_{i=0}^j z_i 2^i + 1 - 2^n \tilde{\delta}}{2^j} \right] \\ \subseteq \left[\frac{z_j 2^j}{2^j}, \frac{z_j 2^j + 2^j - 2^n \tilde{\delta}}{2^j} \right] \subseteq [z_j, z_j + 1 - \tilde{\delta}].$$

744 It follows that

$$745 \quad \phi_0 \left(\frac{x - \sum_{i=j+1}^{n-1} z_i 2^i}{2^j} \right) = z_j \quad \text{for } j = 0, 1, \dots, n-1.$$

746 Therefore, the desired function ϕ can be realized by the network in Figure 14.

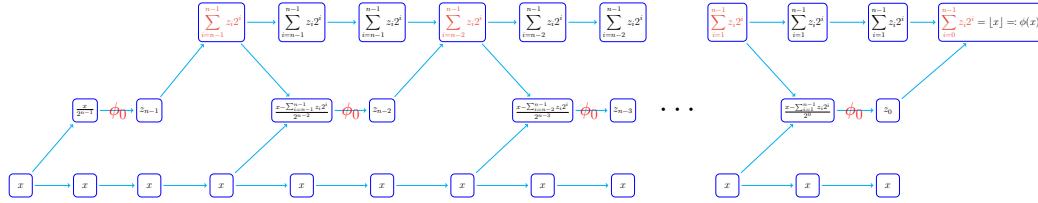


Figure 14: An illustration of the NestNet realizing ϕ . Here, ϕ_0 represent an one-hidden-layer ReLU network of width 2.

747 Clearly,

$$748 \quad \phi(x) = \lfloor x \rfloor \quad \text{for any } x \in \bigcup_{\ell=0}^{2^n-1} [\ell, \ell+1-\delta].$$

749 Moreover, ϕ can be realized by a ReLU network of width $1 + 2 + 1 = 4$ and depth $(1 + 1 + 1) + (1 + 1 + 1)(n-1) = 4n-1$. Hence, we finish the proof of Lemma C.2. \square

751 Next, we introduce the following lemma for the induction step of proving Lemma C.1.

752 **Lemma C.3.** Given any $n, s, \widehat{n} \in \mathbb{N}^+$ and $\delta \in (0, \frac{1}{2^{n,s+1}})$, if $g \in \mathcal{N}_s\{\widehat{n}\}$ satisfying

$$753 \quad g(x) = \lfloor x \rfloor \quad \text{for any } x \in \bigcup_{\ell=0}^{2^{n^s}-1} [\ell, \ell+1-\delta].$$

754 then there exists $\phi \in \mathcal{N}_{s+1}\{\widehat{n} + 12n - 7\}$ such that

$$755 \quad \phi(x) = \lfloor x \rfloor \quad \text{for any } x \in \bigcup_{\ell=0}^{2^{n^{s+1}}-1} [\ell, \ell+1-2^{n^{s+1}}\delta].$$

756 *Proof.* By setting $m = 2^{n^s}$, we have $m^n = (2^{n^s})^n = 2^{(n^s)n} = 2^{n^{s+1}}$ and

$$757 \quad g(x) = \lfloor x \rfloor \quad \text{for any } x \in \bigcup_{\ell=0}^{m-1} [\ell, \ell+1-\delta]. \quad (12)$$

758 By fixing

$$759 \quad x \in \bigcup_{\ell=0}^{2^{n^{s+1}}-1} [\ell, \ell+1-2^{n^{s+1}}\delta] = \bigcup_{\ell=0}^{m^n-1} [\ell, \ell+1-m^n\delta],$$

we have $\lfloor x \rfloor \in \{0, 1, \dots, m^n - 1\}$, implying that $\lfloor x \rfloor$ can be represented as

$$\lfloor x \rfloor = \sum_{i=0}^{n-1} z_i m^i \quad \text{for } z_0, z_1, \dots, z_{n-1} \in \{0, 1, \dots, m-1\}.$$

Then, for $j = 0, 1, \dots, n-1$, we have

$$\sum_{i=0}^j z_i m^i + 1 \leq z_j m^j + \sum_{i=0}^{j-1} (m-1)m^i + 1 = z_j m^j + m^j,$$

implying

$$\begin{aligned} \frac{x - \sum_{i=j+1}^{n-1} z_i m^i}{m^j} &\in \left[\frac{\lfloor x \rfloor - \sum_{i=j+1}^{n-1} z_i m^i}{m^j}, \frac{\lfloor x \rfloor + 1 - m^n \delta - \sum_{i=j+1}^{n-1} z_i m^i}{m^j} \right] \\ &= \left[\frac{\sum_{i=0}^j z_i m^i}{m^j}, \frac{\sum_{i=0}^j z_i m^i + 1 - m^n \delta}{m^j} \right] \\ &\subseteq \left[\frac{z_j m^j}{m^j}, \frac{z_j m^j + m^j - m^n \delta}{m^j} \right] \subseteq [z_j, z_j + 1 - \delta]. \end{aligned}$$

It follows that

$$g\left(\frac{x - \sum_{i=j+1}^{n-1} z_i m^i}{m^j}\right) = z_j \quad \text{for } j = 0, 1, \dots, n-1.$$

Therefore, the desired function ϕ can be realized by the network in Figure 15.

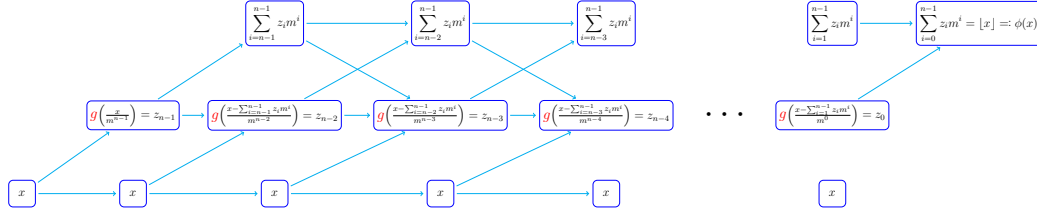


Figure 15: An illustration of the NestNet realizing ϕ . Here, g is regarded as an activation function.

Clearly,

$$\phi(x) = \lfloor x \rfloor \quad \text{for any } x \in \bigcup_{\ell=0}^{m^n-1} [\ell, \ell + 1 - m^n \delta] = \bigcup_{\ell=0}^{2^{n^{s+1}}-1} [\ell, \ell + 1 - 2^{n^{s+1}} \delta].$$

Moreover, the fact $g \in \mathcal{NN}_s\{\widehat{n}\}$ implies that ϕ can be realized by a height- $(s+1)$ NestNet with at most

$$\underbrace{(1+1)2 + (2+1)3 + (3+1)3(n-2) + (3+1)}_{\text{outer network}} + \underbrace{\widehat{n}}_g = \widehat{n} + 12n - 7$$

parameters. Hence, we finish the proof of Lemma C.3. \square

With Lemmas C.2 and C.3 in hand, we are ready to prove Lemma C.1.

Proof of Lemma C.1. We will use the mathematical induction to prove Lemma C.1. First, we consider the base case $r = 1$. By Lemma C.2, there exists a function ϕ realized by a ReLU network of width 4 and depth $4n - 1$ such that

$$\phi(x) = \lfloor x \rfloor \quad \text{for any } x \in \bigcup_{\ell=0}^{2^n-1} [\ell, \ell + 1 - \delta] \subseteq \bigcup_{\ell=0}^{2^n-1} [\ell, \ell + 1 - C(r, n) \cdot \delta] \text{ with } r = 1.$$

Moreover, the network realizing ϕ has at most $(4+1)4((4n-1)+1) = 80n$ parameters, implying $\phi \in \mathcal{NN}_1\{80n\} \subseteq \mathcal{NN}_1\{(12r+68)n\}$ for $r = 1$. Thus, the base case $r = 1$ is proved.

Next, assume Lemma C.1 holds for $r = s \in \mathbb{N}^+$. We need to show it is also true for $r = s+1$. By the induction hypothesis, there exists $g \in \mathcal{NN}_s\{(12s+68)n\}$ such that

$$g(x) = \lfloor x \rfloor \quad \text{for any } x \in \bigcup_{\ell=0}^{2^{n^s}-1} [\ell, \ell + 1 - C(s, n) \cdot \delta].$$

785 By Lemma C.3 with $\widehat{n} = (12s + 68)n$ therein and setting $\widehat{\delta} = C(s, n) \cdot \delta$, there exists

$$786 \quad \phi \in \mathcal{NN}_{s+1}\{\widehat{n} + 12n - 7\} \subseteq \mathcal{NN}_{s+1}\{(12s + 68)n + 12n - 7\} \subseteq \mathcal{NN}_{s+1}\{(12(s + 1) + 68)n\}$$

787 such that

$$788 \quad \phi(x) = \lfloor x \rfloor \quad \text{for any } x \in \bigcup_{\ell=0}^{2^{n^{s+1}}-1} [\ell, \ell + 1 - 2^{n^{s+1}}\widehat{\delta}].$$

789 Observe that

$$790 \quad 2^{n^{s+1}}\widehat{\delta} = 2^{n^{s+1}}C(s, n) \cdot \delta = 2^{n^{s+1}}\left(\prod_{i=1}^s 2^{n^i}\right) \cdot \delta = \left(\prod_{i=1}^{s+1} 2^{n^i}\right) \cdot \delta = C(s + 1, n) \cdot \delta.$$

791 It follows that

$$792 \quad \phi(x) = \lfloor x \rfloor \quad \text{for any } x \in \bigcup_{\ell=0}^{2^{n^{s+1}}-1} [\ell, \ell + 1 - C(s + 1, n) \cdot \delta].$$

793 Thus, Lemma C.1 is proved for the case $r = s + 1$, which means we finish the induction step. Hence,
794 by the principle of induction, we complete the proof of Lemma C.1. \square

795 C.2 Detailed proof of Proposition B.1

796 Set $C(r, n) = \prod_{i=1}^r 2^{n^i}$ and $\widetilde{\delta} = \frac{\delta}{C(r, n)} \in (0, \frac{1}{C(r, n)})$. By Lemma C.1, there exists $\phi_0 \in \mathcal{NN}_r\{(12r +$
797 $68)n\}$ such that

$$798 \quad \phi_0(x) = \lfloor x \rfloor \quad \text{for any } x \in \bigcup_{\ell=0}^{2^{n^r}-1} [\ell, \ell + 1 - C(r, n) \cdot \widetilde{\delta}] = \bigcup_{\ell=0}^{2^{n^r}-1} [\ell, \ell + 1 - \delta].$$

799 It follows from $J \leq 2^{n^r}$ that

$$800 \quad \phi_0(x) = \lfloor x \rfloor \quad \text{for any } x \in \bigcup_{j=0}^{J-1} [j, j + 1 - \delta].$$

801 Set

$$802 \quad \widetilde{M} = \max_{x \in [J, J+1]} |\phi_0(x)| \quad \text{and} \quad M = \frac{\widetilde{M} + J}{\delta}.$$

803 Then, for any $x \in [J, J + 1]$, we have

$$804 \quad \phi_0(x) + M\sigma(x - (J - \delta)) \geq -\widetilde{M} + M\delta = -\widetilde{M} + (\widetilde{M} + J) = J,$$

805 implying

$$806 \quad \min \left\{ \phi_0(x) + M\sigma(x - (J - \delta)), J \right\} = J.$$

807 Moreover, for any $x \in \bigcup_{j=0}^{J-1} [j, j + 1 - \delta]$, we have $\sigma(x - (J - \delta)) = 0$, implying

$$808 \quad \min \left\{ \phi_0(x) + M\sigma(x - (J - \delta)), J \right\} = \min \left\{ \phi_0(x), J \right\} = \min \left\{ \lfloor x \rfloor, J \right\} = \lfloor x \rfloor.$$

809 Therefore, by defining

$$810 \quad \phi(x) := \min \left\{ \phi_0(x) + M\sigma(x - (J - \delta)), J \right\} \quad \text{for any } x \in \bigcup_{j=0}^J [j, j + 1 - \delta \cdot \mathbb{1}_{\{j \leq J-1\}}],$$

811 we have

$$812 \quad \phi(x) = \lfloor x \rfloor \quad \text{for any } x \in \bigcup_{j=0}^{J-1} [j, j + 1 - \delta]$$

813 and

$$814 \quad \phi(x) = J \quad \text{for any } x \in [J, J + 1].$$

815 Moreover, ϕ can be realized by the network in Figure 16. The fact $\phi_0 \in \mathcal{NN}_r\{(12r + 68)n\}$ implies
816 that ϕ can be realized by a height- r NestNet with at most

$$817 \quad \underbrace{3((12r + 68)n)}_{\text{Block 1}} + \underbrace{(2 + 1)4 + (4 + 1)}_{\text{Block 2}} \leq 36(r + 7)n$$

818 parameters. So we finish the proof of Proposition B.1.

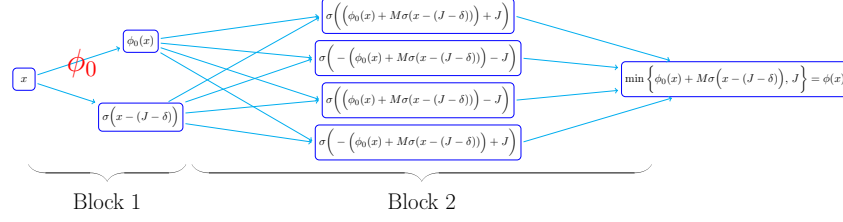


Figure 16: An illustration of the network realizing ϕ for any $x \in \bigcup_{j=0}^J [j, j+1 - \delta \cdot \mathbb{1}_{\{j \leq J-1\}}]$ based on the fact $\min\{a, b\} = \frac{1}{2}(\sigma(a+b) - \sigma(-a-b) - \sigma(a-b) - \sigma(-a+b))$.

819 D Proof of Proposition B.2

820 The key idea of proving Proposition B.2 is the bit extraction technique proposed in [6]. First, we
 821 establish several lemmas for proving Proposition B.2 and give their proofs in Section D.1 except for
 822 Lemma D.2, the proof of which is placed in Section D.3 since it is complicated. Next, we present the
 823 detailed proof of Proposition B.2 in Section D.2 based on the lemmas established in Section D.1.

824 D.1 Lemmas for proving Proposition B.2

825 To simplify the proof of Proposition B.2, we establish several lemmas as the intermediate step. We
 826 first establish a lemma to show that any continuous piecewise linear functions on \mathbb{R} can be realized
 827 by one-hidden-layer ReLU networks.

828 **Lemma D.1.** *Given any $p \in \mathbb{N}^+$, any continuous piecewise linear function on \mathbb{R} with at most p*
 829 *breakpoints can be realized by a one-hidden-layer ReLU network of width $p+1$.*

830 *Proof.* We will use the mathematical induction to prove Lemma D.1. First, we consider the base
 831 case $p=1$. Suppose $f: \mathbb{R} \rightarrow \mathbb{R}$ is a continuous piecewise linear function on \mathbb{R} with at most $p=1$
 832 breakpoints. Then there exist $a_1, a_2, x_0 \in \mathbb{R}$ such that

$$833 \quad f(x) = \begin{cases} a_1(x - x_0) + f(x_0) & \text{if } x \geq x_0 \\ a_2(x_0 - x) + f(x_0) & \text{if } x < x_0. \end{cases}$$

834 Thus, $f(x) = a_1\sigma(x - x_0) + a_2\sigma(x_0 - x) + f(x_0)$ for any $x \in \mathbb{R}$, implying f can be realized by a
 835 one-hidden-layer ReLU network of width $2 = p+1$ for $p=1$. Hence, Lemma D.1 is proved for the
 836 case $p=1$.

837 Now, assume Lemma D.1 holds for $p=k \in \mathbb{N}^+$, we would like to show it is also true for $p=k+1$.
 838 Suppose $f: \mathbb{R} \rightarrow \mathbb{R}$ is a continuous piecewise linear function on \mathbb{R} with at most $k+1$ breakpoints. We
 839 may assume the biggest breakpoint of f is x_0 since it is trivial for the case that f has no breakpoint.
 840 Denote the slopes of the linear pieces left and right next to x_0 by a_1 and a_2 , respectively. Define

$$841 \quad \tilde{f}(x) := f(x) - (a_2 - a_1)\sigma(x - x_0) \quad \text{for any } x \in \mathbb{R}.$$

842 Then \tilde{f} has at most k breakpoints. By the induction hypothesis, \tilde{f} can be realized by a one-hidden-
 843 layer ReLU network of width $k+1$. Thus, there exist $w_{0,j}, b_{0,j}, w_{1,j}, b_1$ for $j=1, 2, \dots, k+1$ such
 844 that

$$845 \quad \tilde{f}(x) = \sum_{j=1}^{k+1} w_{1,j}\sigma(w_{0,j}x + b_{0,j}) + b_1 \quad \text{for any } x \in \mathbb{R}.$$

846 Therefore, for any $x \in \mathbb{R}$, we have

$$847 \quad f(x) = (a_2 - a_1)\sigma(x - x_0) + \tilde{f}(x) = (a_2 - a_1)\sigma(x - x_0) + \sum_{j=1}^{k+1} w_{1,j}\sigma(w_{0,j}x + b_{0,j}) + b_1,$$

848 implying f can be realized by a one-hidden-layer ReLU network of width $k+2 = (k+1) + 1 = p+1$
 849 for $p=k+1$. Thus, we finish the induction process. Therefore, by the principle of induction, we
 850 complete the proof of Lemma D.1. \square

851 Next, we establish a lemma to extract the sum of n^s bits via a height- s NestNet with $\mathcal{O}(n)$ parameters.

852 **Lemma D.2.** Given any $n, s \in \mathbb{N}^+$, there exists $\phi \in \mathcal{NN}_s\{57(s+7)^2(n+1)\}$ such that: For any
 853 $\theta_1, \theta_2, \dots, \theta_{n^s} \in \{0, 1\}$, we have

$$854 \quad \phi(k + \text{bin } 0.\theta_1\theta_2\cdots\theta_{n^s}) = \sum_{\ell=1}^k \theta_\ell \quad \text{for } k = 0, 1, \dots, n^s. \quad (13)$$

855 The proof of Lemma D.2 is complicated, and hence is placed in Section D.3. Then, based on
 856 Lemma D.2, we establish a new lemma, Lemma D.3 below, which is a key intermediate conclusion
 857 to prove Proposition B.2.

858 **Lemma D.3.** Given any $n, s \in \mathbb{N}^+$ and $\theta_{i,\ell} \in \{0, 1\}$ for $i = 0, 1, \dots, n-1$ and $\ell = 0, 1, \dots, m-1$, where
 859 $m = n^s$, there exists $\phi \in \mathcal{NN}_s\{58(s+7)^2(n+1)\}$ such that

$$860 \quad \phi(j) = \sum_{\ell=0}^k \theta_{i,\ell} \quad \text{for } j = 0, 1, \dots, nm-1,$$

861 where (i, k) is the unique index pair satisfying $j = im + k$ with $i \in \{0, 1, \dots, n-1\}$ and $k \in$
 862 $\{0, 1, \dots, m-1\}$.

863 *Proof.* We first construct a network to extract the unique index pair (i, k) from $j \in \{0, 1, \dots, nm-1\}$
 864 with the following condition

$$865 \quad j = im + k \quad \text{with } i \in \{0, 1, \dots, n-1\} \text{ and } k \in \{0, 1, \dots, m-1\}.$$

866 There exists a continuous piecewise linear function ϕ_1 with $2n$ breakpoints such that

$$867 \quad \phi_1(x) = \lfloor x \rfloor \quad \text{for any } x \in \bigcup_{\ell=0}^{n-1} [\ell, \ell+1-\delta] \text{ with } \delta = \frac{1}{2m}.$$

868 By Lemma D.1, ϕ_1 can be realized by a one-hidden-layer ReLU network of width $2n+1$. Moreover,
 869 for any $j \in \{0, 1, \dots, nm-1\}$, we have

$$870 \quad \phi_1\left(\frac{j}{m}\right) = \lfloor \frac{j}{m} \rfloor = i \quad \text{and} \quad j - m\phi_1\left(\frac{j}{m}\right) = j - mi = k,$$

871 where (i, k) is the unique index pair satisfying $j = im + k$ with $i \in \{0, 1, \dots, n-1\}$ and $k \in$
 872 $\{0, 1, \dots, m-1\}$. By defining

$$873 \quad \Phi_1(x) := \begin{bmatrix} \phi_1\left(\frac{x}{m}\right) \\ x - m\phi_1\left(\frac{x}{m}\right) \end{bmatrix} \quad \text{for any } x \geq 0,$$

874 we have

$$875 \quad \Phi_1(j) = \begin{bmatrix} \phi_1\left(\frac{j}{m}\right) \\ j - m\phi_1\left(\frac{j}{m}\right) \end{bmatrix} = \begin{bmatrix} i \\ k \end{bmatrix} \quad \text{for } j = 0, 1, \dots, nm-1,$$

876 where (i, k) is the unique index pair satisfying $j = im + k$ with $i \in \{0, 1, \dots, n-1\}$ and $k \in \{0, 1, \dots, m-$
 877 $1\}$. Moreover, Φ_1 can be realized by a one-hidden-layer ReLU network of width $2(2n+1)+1 = 4n+3$.
 878 Hence, the network realizing Φ_1 has at most $(1+1)(4n+3) + ((4n+3)+1)2 = 16n+14$ parameters.

879 Define

$$880 \quad z_i := \text{bin } 0.\theta_{i,0}\theta_{i,1}\cdots\theta_{i,m-1} \quad \text{for } i = 0, 1, \dots, n-1.$$

881 There exists a continuous piecewise linear function $\tilde{\phi}_2$ with n breakpoints such that

$$882 \quad \tilde{\phi}_2(i) = z_i \quad \text{for } i = 0, 1, \dots, n-1.$$

883 By Lemma D.1, $\tilde{\phi}_2$ can be realized by a one-hidden-layer ReLU network of width $n+1$.

884 By Lemma D.2, there exists $\phi_3 \in \mathcal{NN}_s\{57(s+7)^2(n+1)\}$ such that: For any $\xi_1, \xi_2, \dots, \xi_{n^s} \in \{0, 1\}$,
 885 we have

$$886 \quad \phi_3(k + \text{bin } 0.\xi_1\xi_2\cdots\xi_{n^s}) = \sum_{\ell=1}^k \xi_\ell \quad \text{for } k = 1, 2, \dots, n^s.$$

887 It follows from $m = n^s$ that, for any $\xi_0, \xi_1, \dots, \xi_{m-1} \in \{0, 1\}$, we have

$$888 \quad \phi_3(k + \text{bin } 0.\xi_0\xi_1\cdots\xi_{m-1}) = \sum_{\ell=1}^k \xi_{\ell-1} = \sum_{\ell=0}^{k-1} \xi_\ell \quad \text{for } k = 1, 2, \dots, m,$$

889 implying

$$890 \quad \phi_3(k+1 + \text{bin} 0.\xi_0\xi_1\cdots\xi_{m-1}) = \sum_{\ell=0}^k \xi_\ell \quad \text{for } k = 0, 1, \dots, m-1.$$

891 Then, for $i = 0, 1, \dots, n-1$ and $k = 0, 1, \dots, m-1$, we have

$$892 \quad \phi_3(k+1 + \widetilde{\phi}_2(i)) = \phi_2(k+1 + z_i) = \phi_3(k+1 + \text{bin} 0.\theta_{i,0}\theta_{i,1}\cdots\theta_{i,m-1}) = \sum_{\ell=0}^k \theta_{i,\ell}.$$

893 By defining

$$894 \quad \phi_2(x, y) := y + 1 + \widetilde{\phi}_2(x) \quad \text{for any } x, y \in [0, \infty)$$

895 and $\phi := \phi_3 \circ \phi_2 \circ \Phi_1$, we have

$$896 \quad \phi(j) = \phi_3 \circ \phi_2 \circ \Phi_1(j) = \phi_3 \circ \phi_2(i, k) = \phi_3(k+1 + \widetilde{\phi}_2(i)) = \sum_{\ell=0}^k \theta_{i,\ell}$$

897 for $j = 0, 1, \dots, nm-1$, where (i, k) is the unique index pair satisfying $j = im + k$ with $i \in$
898 $\{0, 1, \dots, n-1\}$ and $k \in \{0, 1, \dots, m-1\}$.

899 It remains to estimate the number of parameters in the NestNet realizing $\phi = \phi_3 \circ \phi_2 \circ \Phi_1$. Observe
900 that ϕ_2 can be realized by a one-hidden-layer ReLU network of width $(n+1) + 1 = n+2$. Then, the
901 network realizing ϕ_2 has at most $(2+1)(n+2) + ((n+2)+1) = 4n+9$ parameters. Therefore, ϕ
902 can be realized by a height- s NestNet with at most

$$903 \quad \underbrace{(16n+14)}_{\Phi_1} + \underbrace{(4n+9)}_{\phi_2} + \underbrace{57(s+7)^2(n+1)}_{\phi_3} \leq 58(s+7)^2(n+1)$$

904 parameters, which means we complete the proof of Lemma D.3. \square

905 D.2 Detailed proof of Proposition B.2

906 We may assume $J = mn = n^{s+1}$ with $m = n^s$ since we can set $y_{J-1} = y_J = \cdots = y_{mn-1}$ if $J < mn$.
907 Define

$$908 \quad a_j := \lfloor y_j / \varepsilon \rfloor \quad \text{for } j = 0, 1, \dots, nm-1.$$

909 Our goal is to construct a function ϕ such that $\phi(j) = a_j \varepsilon$ for $j = 0, 1, \dots, nm-1$.

910 For $i = 0, 1, \dots, n-1$, we define

$$911 \quad b_{i,\ell} = \begin{cases} 0 & \text{for } \ell = 0 \\ a_{im+\ell} - a_{im+\ell-1} & \text{for } \ell = 1, 2, \dots, m-1. \end{cases}$$

912 Since $|y_j - y_{j-1}| \leq \varepsilon$ for all j , we have $|a_j - a_{j-1}| \leq 1$. It follows that $b_{i,\ell} \in \{-1, 0, 1\}$ for $i =$
913 $0, 1, \dots, n-1$ and $\ell = 0, 1, \dots, m-1$. Hence, there exist $c_{i,\ell} \in \{0, 1\}$ and $d_{i,\ell} \in \{0, 1\}$ such that

$$914 \quad b_{i,\ell} = c_{i,\ell} - d_{i,\ell} \quad \text{for } i = 0, 1, \dots, n-1 \text{ and } \ell = 0, 1, \dots, m-1.$$

915 Since any $j \in \{0, 1, \dots, nm-1\}$ can be uniquely indexed as $j = im + k$ with $i \in \{0, 1, \dots, n-1\}$ and
916 $k \in \{0, 1, \dots, m-1\}$, we have

$$\begin{aligned} 917 \quad a_j &= a_{im+k} = a_{im} + \sum_{\ell=1}^k (a_{im+\ell} - a_{im+\ell-1}) = a_{im} + \sum_{\ell=1}^k b_{i,\ell} = a_{im} + \sum_{\ell=0}^k b_{i,\ell} \\ &= a_{im} + \sum_{\ell=0}^k c_{i,\ell} - \sum_{\ell=0}^k d_{i,\ell}. \end{aligned}$$

918 There exists a continuous piecewise linear function ϕ_1 with $2n$ breakpoints such that

$$919 \quad \phi_1(x) = a_{im} \quad \text{for any } x \in [im, im+m-1] \text{ and } i = 0, 1, \dots, n-1.$$

920 Then, we have

$$921 \quad \phi_1(j) = a_{im} \quad \text{for } j = 0, 1, \dots, nm-1,$$

where (i, k) is the unique index pair satisfying $j = im + k$ with $i \in \{0, 1, \dots, n-1\}$ and $k \in \{0, 1, \dots, m-1\}$. By Lemma D.1, ϕ_1 can be realized by a one-hidden-layer ReLU network of width $2n+1$.

By Lemma D.3, there exist $\phi_2, \phi_3 \in \mathcal{N}_s\{58(s+7)^2(n+1)\}$ such that

$$\phi_2(j) = \sum_{\ell=0}^k c_{i,\ell} \quad \text{and} \quad \phi_3(j) = \sum_{\ell=0}^k d_{i,\ell} \quad \text{for } j = 0, 1, \dots, nm-1,$$

where (i, k) is the unique index pair satisfying $j = im + k$ with $i \in \{0, 1, \dots, n-1\}$ and $k \in \{0, 1, \dots, m-1\}$.

Hence, by indexing $j \in \{0, 1, \dots, nm-1\}$ as $j = im + k$ for $i \in \{0, 1, \dots, n-1\}$ and $k \in \{0, 1, \dots, m-1\}$, we have

$$a_j = a_{im} + \sum_{\ell=0}^k c_{i,\ell} - \sum_{\ell=0}^k d_{i,\ell} = \phi_1(j) + \phi_2(j) - \phi_3(j).$$

By defining

$$\tilde{\phi}(x) := (\phi_1(x) + \phi_2(x) + \phi_3(x))\varepsilon \quad \text{for any } x \in \mathbb{R},$$

we have $\tilde{\phi}(j) = a_j\varepsilon$ for $j = 0, 1, \dots, nm-1$ and $\tilde{\phi}$ can be realized by the height- s NestNet in Figure 17.

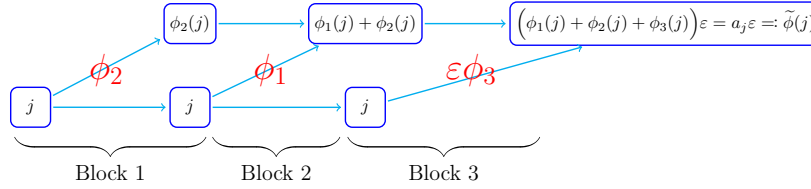


Figure 17: An illustration of the NestNet realizing $\tilde{\phi}$ for $j = 0, 1, \dots, J-1$.

In Figure 17, Block 1 or 3 has at most

$$3(58(s+7)^2(n+1)) = 174(s+7)^2(n+1)$$

parameters; Block 2 is of width $(2n+1) + 2 = 2n+3$ and depth 1, and hence has at most

$$(2+1)(2n+3) + ((2n+3)+1)2 = 10n+17$$

parameters. Then, $\tilde{\phi}$ can be realized by a height- s ReLU NestNet with at most

$$2(174(s+7)^2(n+1)) + 10n+17 = 349(s+7)^2(n+1)$$

parameters. Note that $\tilde{\phi}$ may not be bounded. Thus, we define

$$\psi(x) := \min\{\sigma(x), M\} \quad \text{for any } x \in \mathbb{R},$$

where

$$M = \max\{y_j : j = 0, 1, \dots, nm-1\}.$$

Then, the desired function ϕ can be define via $\phi := \psi \circ \tilde{\phi}$. Clearly,

$$0 \leq \phi(x) \leq M = \max\{y_j : j = 0, 1, \dots, J-1\} \quad \text{for any } x \in \mathbb{R}.$$

It follows from $0 \leq a_j\varepsilon = \lfloor y_j/\varepsilon \rfloor \varepsilon \leq y_j \leq M$ for $j = 0, 1, \dots, J-1$ that

$$\phi(j) = \psi \circ \tilde{\phi}(j) = \psi(a_j\varepsilon) = \min\{\sigma(a_j\varepsilon), M\} = a_j\varepsilon,$$

implying

$$|\phi(j) - y_j| = |a_j\varepsilon - y_j| = |\lfloor y_j/\varepsilon \rfloor \varepsilon - y_j| = |\lfloor y_j/\varepsilon \rfloor - y_j/\varepsilon| \varepsilon \leq \varepsilon.$$

It remains to show that ϕ can be realized by a height- s ReLU NestNet with the desired size. Clearly, ψ can be realized by the network in Figure 18, which is of width 4 and depth 2.

Therefore, ϕ can be realized by a height- s ReLU NestNet with at most

$$349(s+7)^2(n+1) + (4+1)4(2+1) \leq 350(s+7)^2(n+1)$$

parameters. Hence, we finish the proof of Proposition B.2.

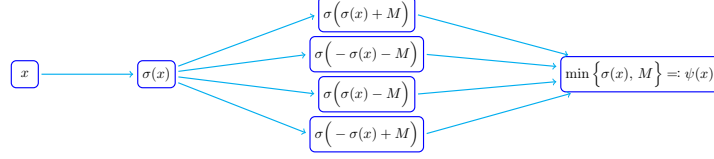


Figure 18: An illustration of the network realizing ψ based on the fact $\min\{a, b\} = \frac{1}{2}(\sigma(a+b) - \sigma(-a-b) - \sigma(a-b) - \sigma(-a+b))$.

956 D.3 Proof of Lemma D.2 for Proposition B.2

957 We will use the mathematical induction to prove Lemma D.2. To this end, we introduce two lemmas
958 for the base case and the induction step.

959 **Lemma D.4.** *Given any $n \in \mathbb{N}^+$, there exists a function ϕ realized by a ReLU network with $128n + 294$
960 parameters such that: For any $\theta_1, \theta_2, \dots, \theta_n \in \{0, 1\}$, we have*

$$961 \quad \phi(k + \text{bin } 0.\theta_1\theta_2\cdots\theta_n) = \sum_{\ell=1}^k \theta_\ell \quad \text{for } k = 0, 1, \dots, n. \quad (14)$$

962 **Lemma D.5.** *Given any $n, r, \widehat{n} \in \mathbb{N}^+$, if $g \in \mathcal{NN}_r\{\widehat{n}\}$ satisfying*

$$963 \quad g(p + \text{bin } 0.\xi_1\xi_2\cdots\xi_{n^r}) = \sum_{j=1}^p \xi_j \quad \text{for any } \xi_1, \xi_2, \dots, \xi_{n^r} \in \{0, 1\} \text{ and } p = 0, 1, \dots, n^r, \quad (15)$$

964 *then there exists $\phi \in \mathcal{NN}_{r+1}\{\widehat{n} + 114(r+7)(n+1)\}$ such that: For any $\theta_1, \theta_2, \dots, \theta_{n^{r+1}} \in \{0, 1\}$, we
965 have*

$$966 \quad \phi(k + \text{bin } 0.\theta_1\theta_2\cdots\theta_{n^{r+1}}) = \sum_{\ell=1}^k \theta_\ell \quad \text{for } k = 0, 1, \dots, n^{r+1}.$$

967 The proofs of Lemmas D.4 and D.5 can be found in Sections D.3.1 and D.3.2, respectively. Remark
968 that the function ϕ in Lemma D.5 is independent of $\theta_1, \theta_2, \dots, \theta_{nm}$. The proof of Lemma D.2 mainly
969 relies on Lemma D.4 and repeated applications of Lemma D.5. The details can be found below.

970 *Proof of Lemma D.2.* We will use the mathematical induction to prove Lemma D.2. First, let us
971 consider the base case $s = 1$. By Lemma D.4, there exists a function realized by a ReLU network
972 with $128n + 294$ parameters such that: For any $\theta_1, \theta_2, \dots, \theta_n \in \{0, 1\}$, we have

$$973 \quad \phi(k + \text{bin } 0.\theta_1\theta_2\cdots\theta_n) = \sum_{\ell=1}^k \theta_\ell \quad \text{for } k = 0, 1, \dots, n.$$

974 That means Equation (13) holds for $s = 1$. Moreover, ϕ can also be regarded as a height-1 ReLU
975 NestNet with $128n + 294 \leq 57(s+7)^2(n+1)$ parameters for $s = 1$, which means Lemma D.2 is
976 proved for the case $s = 1$.

977 Next, assume Lemma D.2 holds for $s = r \in \mathbb{N}^+$. We need to show that it is also true for $s = r + 1$ by
978 applying Lemma D.5. By the induction hypothesis, there exists

$$979 \quad g \in \mathcal{NN}_r\{57(r+7)^2(n+1)\}$$

980 such that: For any $\xi_1, \xi_2, \dots, \xi_{n^r} \in \{0, 1\}$, we have

$$981 \quad g(k + \text{bin } 0.\xi_1\xi_2\cdots\xi_{n^r}) = \sum_{\ell=1}^k \xi_\ell \quad \text{for } k = 0, 1, \dots, n^r.$$

982 It follows from $m = n^r$ that

$$983 \quad g(p + \text{bin } 0.\xi_1\xi_2\cdots\xi_m) = \sum_{j=1}^p \xi_j \quad \text{for any } \xi_1, \xi_2, \dots, \xi_m \in \{0, 1\} \text{ and } p = 0, 1, \dots, m,$$

984 which means g satisfies Equation (15). Then, by Lemma D.5 with $m = n^r$ and $\widehat{n} = 57(r+7)^2(n+1)$
 985 therein, there exists

$$986 \quad \phi \in \mathcal{NN}_{r+1} \left\{ \widehat{n} + 114(r+7)(n+1) \right\}$$

987 such that: For any $\theta_1, \theta_2, \dots, \theta_{nm} \in \{0, 1\}$, we have

$$988 \quad \phi(k + \text{bin } 0.\theta_1\theta_2\cdots\theta_{nm}) = \sum_{\ell=1}^k \theta_\ell \quad \text{for } k = 0, 1, \dots, nm.$$

989 It follows from $m = n^r$ that, for any $\theta_1, \theta_2, \dots, \theta_{n^{r+1}} \in \{0, 1\}$, we have

$$990 \quad \phi(k + \text{bin } 0.\theta_1\theta_2\cdots\theta_{n^{r+1}}) = \sum_{\ell=1}^k \theta_\ell \quad \text{for } k = 0, 1, \dots, n^{r+1},$$

991 which means Equation (13) holds for $s = r + 1$. Moreover, we have

$$\begin{aligned} \widehat{n} + 114(r+7)(n+1) &= 57(r+7)^2(n+1) + 114(r+7)(n+1) \\ &= 57(n+1)((r+7)^2 + 2(r+7)) \\ &\leq 57(n+1)((r+7)+1)^2 = 57((r+1)+7)^2(n+1). \end{aligned}$$

993 This implies that

$$994 \quad \phi \in \mathcal{NN}_{r+1} \left\{ \widehat{n} + 114(r+7)(n+1) \right\} \subseteq \mathcal{NN}_{r+1} \left\{ 57((r+1)+7)^2(n+1) \right\}.$$

995 Thus, we prove Lemma D.2 for the case $s = r + 1$, which means we finish the induction step. Hence,
 996 by the principle of induction, we complete the proof of Lemma D.2. \square

997 D.3.1 Proof of Lemma D.4 for Lemma D.2

998 To simplify the proof of Lemma D.4, we introduce the following lemma.

999 **Lemma D.6.** *Given any $n \in \mathbb{N}^+$, there exists a function ϕ realized by a ReLU network of width 7 and*
 1000 *depth $2n + 1$ such that: For any $\theta_1, \theta_2, \dots, \theta_n \in \{0, 1\}$, we have*

$$1001 \quad \phi(\text{bin } 0.\theta_1\theta_2\cdots\theta_n, k) = \sum_{\ell=1}^k \theta_\ell \quad \text{for } k = 0, 1, \dots, n.$$

1002 Lemma D.6 is the Lemma 3.5 of [33]. The detailed proof can be found therein. With Lemma D.6 in
 1003 hand, we are ready to prove Lemma D.4.

1004 *Proof of Lemma D.4.* By Lemma D.6, there exists a function ϕ_0 realized by a ReLU network of
 1005 width 7 and depth $2n + 1$ such that: For any $\theta_1, \theta_2, \dots, \theta_n \in \{0, 1\}$, we have

$$1006 \quad \phi_0(\text{bin } 0.\theta_1\theta_2\cdots\theta_n, k) = \sum_{\ell=1}^k \theta_\ell \quad \text{for } k = 1, 2, \dots, n.$$

1007 The equation above is not true for $k = 0$. We will construct ϕ_2 such that

$$1008 \quad \phi_2(\text{bin } 0.\theta_1\theta_2\cdots\theta_n, k) = \sum_{\ell=1}^k \theta_\ell \quad \text{for } k = 0, 1, \dots, n.$$

1009 To this end, we first set

$$1010 \quad M = \max \{ |\phi_0(x, y)| : x \in [0, 1], y \in [0, n] \}$$

1011 and define

$$1012 \quad \phi_1(x, y) := \min \{ M + \phi_0(x, y), 2My \} \quad \text{for any } x \in [0, 1] \text{ and } y \in [0, n].$$

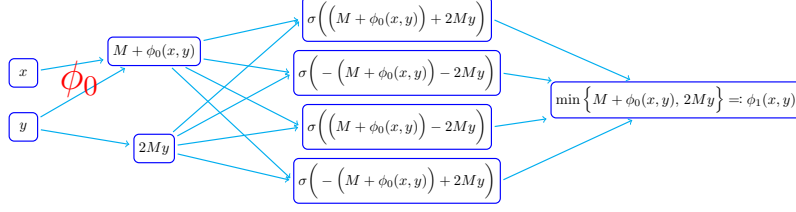


Figure 19: An illustration of the network realizing ϕ_1 for any $x \in [0, 1]$ and $y \in [0, n]$ based on the fact $\min\{a, b\} = \frac{1}{2}(\sigma(a+b) - \sigma(-a-b) - \sigma(a-b) - \sigma(-a+b))$.

1013 As we can see from Figure 19, ϕ_1 can be realized by a ReLU network of width $\max\{7, 4\} = 7$ and
 1014 depth $(2n+1) + 2 = 2n+3$. Moreover, we have

$$\begin{aligned} \phi_1(\text{bin } 0.\theta_1\theta_2\cdots\theta_n, k) &= \min\{M + \phi_0(\text{bin } 0.\theta_1\theta_2\cdots\theta_n, k), 2Mk\} \\ &= \begin{cases} M + \sum_{\ell=1}^k \theta_\ell & \text{for } k = 1, 2, \dots, n \\ 0 & \text{for } k = 0. \end{cases} \end{aligned}$$

1016 Define

$$\phi_2(x, y) := \sigma(\phi_1(x, y) - M) \quad \text{for any } x \in [0, 1] \text{ and } y \in [0, \infty).$$

1017 Then, ϕ_2 can be realized by a ReLU network of width 7 and depth $(2n+3) + 1 = 2n+4$. Moreover,
 1018 we have

$$\begin{aligned} \phi_2(\text{bin } 0.\theta_1\theta_2\cdots\theta_n, k) &= \sigma(\phi_1(\text{bin } 0.\theta_1\theta_2\cdots\theta_n, k) - M) \\ &= \begin{cases} \sigma(\sum_{\ell=1}^k \theta_\ell) = \sum_{\ell=1}^k \theta_\ell & \text{for } k = 1, 2, \dots, n \\ \sigma(-M) = 0 & \text{for } k = 0. \end{cases} \end{aligned}$$

1021 That is,

$$\phi_2(\text{bin } 0.\theta_1\theta_2\cdots\theta_n, k) = \sum_{\ell=1}^k \theta_\ell \quad \text{for } k = 0, 1, \dots, n.$$

1023 Next, we will construct Ψ to extract k and $\text{bin } 0.\theta_1\theta_2\cdots\theta_n$ from $k + \text{bin } 0.\theta_1\theta_2\cdots\theta_n$. It is easy to
 1024 construct a continuous piecewise linear function $\psi : \mathbb{R} \rightarrow \mathbb{R}$ with $2n$ breakpoints satisfying

$$\psi(x) = \lfloor x \rfloor \quad \text{for any } x \in \bigcup_{\ell=0}^{n-1} [\ell, \ell+1-\delta] \text{ with } \delta = 2^{-n}.$$

1026 By Lemma D.1 with $p = 2n$ therein, ψ can be realized by a one-hidden-layer ReLU network of width
 1027 $2n+1$. By defining

$$\Psi(x) := \begin{bmatrix} x - \psi(x) \\ \psi(x) \end{bmatrix} = \begin{bmatrix} \sigma(x) - \psi(x) \\ \psi(x) \end{bmatrix} \quad \text{for any } x \in [0, \infty).$$

1029 Then, Ψ can be realized by a one-hidden-layer ReLU network of width $1 + 2(2n+1) = 4n+3$. That
 1030 means, the network realizing Ψ has at most

$$(1+1)(4n+3) + ((4n+3)+1)2 = 16n+14$$

1032 parameters. Moreover, for any $\theta_1, \theta_2, \dots, \theta_n \in \{0, 1\}$ and $k = 0, 1, \dots, n$, we have

$$\psi(k + \text{bin } 0.\theta_1\theta_2\cdots\theta_n) = \lfloor k + \text{bin } 0.\theta_1\theta_2\cdots\theta_n \rfloor = k,$$

1034 implying

$$\begin{aligned} \Psi(k + \text{bin } 0.\theta_1\theta_2\cdots\theta_n) &= \begin{bmatrix} k + \text{bin } 0.\theta_1\theta_2\cdots\theta_n - \psi(k + \text{bin } 0.\theta_1\theta_2\cdots\theta_n) \\ \psi(k + \text{bin } 0.\theta_1\theta_2\cdots\theta_n) \end{bmatrix} \\ &= \begin{bmatrix} \text{bin } 0.\theta_1\theta_2\cdots\theta_n \\ k \end{bmatrix}. \end{aligned}$$

1036 Finally, the desired function ϕ can be defined via $\phi := \phi_2 \circ \Psi$. Clearly, the network realizing ϕ_2 is of
 1037 width 7 and depth $2n+4$, and hence has at most

$$(7+1)7((2n+4)+1) = 56(2n+5)$$

1039 parameters, implying ϕ can be realized by a ReLU network with at most

$$1040 \quad 56(2n + 5) + (16n + 14) = 128n + 294$$

1041 parameters. Moreover, for any $\theta_1, \theta_2, \dots, \theta_n \in \{0, 1\}$ and $k = 0, 1, \dots, n$, we have

$$\begin{aligned} 1042 \quad \phi(k + \text{bin } 0.\theta_1\theta_2\cdots\theta_n) &= \phi_2 \circ \Psi(k + \text{bin } 0.\theta_1\theta_2\cdots\theta_n) \\ &= \phi_2(\text{bin } 0.\theta_1\theta_2\cdots\theta_n, k) = \sum_{\ell=1}^k \theta_\ell. \end{aligned}$$

1043 Thus, we finish the proof of Lemma D.4. \square

1044 D.3.2 Proof of Lemma D.5 for Lemma D.2

1045 The key idea of proving Lemma D.5 is to construct a network with n blocks, each of which extracts
1046 the sum of n^r bits via g . Then the whole network can extract the sum of n^{r+1} bits as we expect.

1047 To simplify our notation, we set $m = n^r$. Given any nm binary bits $\theta_\ell \in \{0, 1\}$ for $\ell = 1, 2, \dots, nm$,
1048 we divide these nm bits into n classes according to their indices, where the i -th class is composed
1049 of m bits $\theta_{im+1}, \dots, \theta_{i(m+1)}$ for $i = 0, 1, \dots, n-1$. We will show how to extract the m bits of the i -th
1050 class, stored in $\text{bin } 0.\theta_{im+1}\cdots\theta_{i(m+1)}$.

1051 First, let us show how to construct a network to extract k and $\text{bin } 0.\theta_1\theta_2\cdots\theta_{nm}$ from $k + 0.\theta_1\theta_2\cdots\theta_{nm}$.
1052 By setting $\tilde{n} = 2n$ and Proposition B.1 with $J = 2^{\tilde{n}^r}$ therein, there exists

$$1053 \quad \tilde{g} \in \mathcal{NN}_r\{36(r+7)\tilde{n}\} = \mathcal{NN}_r\{36(r+7)(2n)\} = \mathcal{NN}_r\{72(r+7)n\}$$

1054 such that

$$1055 \quad \tilde{g}(x) = \lfloor x \rfloor \quad \text{for any } x \in \bigcup_{\ell=0}^{J-1} [\ell, \ell+1-\delta].$$

1056 Observe that

$$1057 \quad J-1 = 2^{\tilde{n}^r} - 1 = 2^{(2n)^r} - 1 \geq 2^{2(n^r)} - 1 = 2^{2m} - 1 = 4^m - 1 \geq m^2 \geq nm.$$

1058 It follows from $\text{bin } 0.\theta_1\theta_2\cdots\theta_{nm} \leq 1 - 2^{-nm} = 1 - \delta$ that

$$1059 \quad k + \text{bin } 0.\theta_1\theta_2\cdots\theta_{nm} \in \bigcup_{\ell=0}^{nm} [\ell, \ell+1-\delta] \subseteq \bigcup_{\ell=0}^{J-1} [\ell, \ell+1-\delta]$$

1060 for $k = 0, 1, \dots, nm$. Thus, we have

$$1061 \quad \tilde{g}(k + \text{bin } 0.\theta_1\theta_2\cdots\theta_{nm}) = k \quad \text{for } k = 0, 1, \dots, nm. \quad (16)$$

1062 It is easy to verify that

$$1063 \quad 2^m \cdot \text{bin } 0.\theta_{im+1}\cdots\theta_{nm} \in \bigcup_{\ell=0}^{2^m-1} [\ell, \ell+1-\delta] \quad \text{for } i = 0, 1, \dots, n-1.$$

1064 Since $2^m - 1 = 2^{n^r} - 1 \leq 2^{(2n)^r} - 1 = J - 1$, we have

$$1065 \quad \tilde{g}(2^m \cdot \text{bin } 0.\theta_{im+1}\cdots\theta_{nm}) = \lfloor 2^m \cdot \text{bin } 0.\theta_{im+1}\cdots\theta_{nm} \rfloor \quad \text{for } i = 0, 1, \dots, n-1.$$

1066 Therefore, for $i = 0, 1, \dots, n-1$, we have

$$1067 \quad \text{bin } 0.\theta_{im+1}\cdots\theta_{i(m+1)} = \frac{\lfloor 2^m \cdot \text{bin } 0.\theta_{im+1}\cdots\theta_{nm} \rfloor}{2^m} = \frac{\tilde{g}(2^m \cdot \text{bin } 0.\theta_{im+1}\cdots\theta_{nm})}{2^m}$$

1068 and

$$\begin{aligned} 1069 \quad \text{bin } 0.\theta_{(i+1)m+1}\cdots\theta_{nm} &= 2^m \left(\text{bin } 0.\theta_{im+1}\cdots\theta_{nm} - \text{bin } 0.\theta_{im+1}\cdots\theta_{i(m+1)} \right) \\ &= 2^m \left(\text{bin } 0.\theta_{im+1}\cdots\theta_{nm} - \frac{\tilde{g}(2^m \cdot \text{bin } 0.\theta_{im+1}\cdots\theta_{nm})}{2^m} \right). \end{aligned}$$

1070 By defining

$$1071 \quad \phi_1(x) := \frac{\tilde{g}(2^m x)}{2^m} \quad \text{and} \quad \phi_2(x) := 2^m \left(x - \frac{\tilde{g}(2^m x)}{2^m} \right) = \left(\sigma(x) - \frac{\tilde{g}(2^m x)}{2^m} \right) \quad \text{for } x \geq 0,$$

1072 we have

$$1073 \quad \text{bin } 0.\theta_{im+1}\cdots\theta_{im+m} = \phi_1(\text{bin } 0.\theta_{im+1}\cdots\theta_{nm}) \quad (17)$$

1074 and

$$1075 \quad \text{bin } 0.\theta_{(i+1)m+1}\cdots\theta_{nm} = \phi_2(\text{bin } 0.\theta_{im+1}\cdots\theta_{nm}) \quad (18)$$

1076 for any $i \in \{0, 1, \dots, n-1\}$. Moreover, ϕ_1 can be realized by a one-hidden-layer \tilde{g} -activated network
1077 of width 1; ϕ_2 can be realized by a one-hidden-layer (σ, \tilde{g}) -activated network of width 2.

1078 Define

$$1079 \quad \phi_{3,i}(x) := \min\{\sigma(x - im), m\} \quad \text{for any } x \in \mathbb{R} \text{ and } i = 0, 1, \dots, n-1.$$

1080 For any $k \in \{1, 2, \dots, nm\}$, there exist $k_1 \in \{0, 1, \dots, n-1\}$ and $k_2 \in \{1, 2, \dots, m\}$ such that $k =$
1081 $k_1m + k_2$. Then we have

$$1082 \quad \phi_{3,i}(k) = \min\{\sigma(k - im), m\} = \begin{cases} m & \text{if } i \leq k_1 - 1 \\ k_2 & \text{if } i = k_1 \\ 0 & \text{if } i \geq k_1 + 1. \end{cases} \quad (19)$$

1083 Observe that

$$1084 \quad \begin{aligned} \{1, 2, \dots, k\} &= \{1, 2, \dots, k_1m + k_2\} \\ &= \left(\bigcup_{i=1}^{k_1-1} \{im + j : j = 1, 2, \dots, m\} \right) \cup \{k_1m + j : j = 1, 2, \dots, k_2\}. \end{aligned}$$

1085 It follows that

$$\begin{aligned} \sum_{\ell=1}^k \theta_{\ell} &= \sum_{\ell=1}^{k_1m+k_2} \theta_{\ell} = \sum_{i=0}^{k_1-1} \left(\sum_{j=1}^m \theta_{im+j} \right) + \sum_{j=1}^{k_2} \theta_{k_1m+j} + 0 \\ &= \sum_{i=0}^{k_1-1} \left(\sum_{j=1}^m \theta_{im+j} \right) + \sum_{i=k_1}^{k_1} \left(\sum_{j=1}^{k_2} \theta_{im+j} \right) + \sum_{i=k_1+1}^{n-1} \left(\sum_{j=1}^0 \theta_{im+j} \right) \\ 1086 \quad &= \sum_{i=0}^{k_1-1} \left(\sum_{j=1}^{\phi_{3,i}(k)} \theta_{im+j} \right) + \sum_{i=k_1}^{k_1} \left(\sum_{j=1}^{\phi_{3,i}(k)} \theta_{im+j} \right) + \sum_{i=k_1+1}^{n-1} \left(\sum_{j=1}^{\phi_{3,i}(k)} \theta_{im+j} \right) \\ &= \sum_{i=0}^{n-1} \left(\sum_{j=1}^{\phi_{3,i}(k)} \theta_{im+j} \right) \end{aligned} \quad (20)$$

1087 for $k \in \{1, 2, \dots, nm\}$, where the second to last equality comes from Equation (19). It is easy to verify
1088 that Equation (20) also holds for $k = 0$, i.e.,

$$1089 \quad \sum_{\ell=1}^0 \theta_{\ell} = 0 = \sum_{i=0}^{n-1} \left(\sum_{j=1}^0 \theta_{im+j} \right) = \sum_{i=0}^{n-1} \left(\sum_{j=1}^{\phi_{3,i}(0)} \theta_{im+j} \right).$$

1090 Therefore, we have

$$1091 \quad \sum_{\ell=1}^k \theta_{\ell} = \sum_{i=0}^{n-1} \left(\sum_{j=1}^{\phi_{3,i}(k)} \theta_{im+j} \right) \quad \text{for any } k \in \{0, 1, \dots, nm\}. \quad (21)$$

1092 Fix $i \in \{0, 1, \dots, n-1\}$. By setting $p = \phi_{3,i}(k) \in \{0, 1, \dots, m\}$ and $\xi_j = \theta_{im+j}$ for $j = 1, 2, \dots, m$ in
1093 Equation (15), we have

$$1094 \quad g(\phi_{3,i}(k) + \text{bin } 0.\theta_{im+1}\theta_{im+2}\cdots\theta_{im+m}) = \sum_{j=1}^{\phi_{3,i}(k)} \theta_{im+j}. \quad (22)$$

1095 With Equations (16), (17), (18), (21), and (22) in hand, we are ready to construct the desired function
1096 ϕ , which can be realized by the NestNet in Figure 20. Clearly, we have

$$1097 \quad \phi(k + \text{bin } 0.\theta_1\cdots\theta_{nm}) = \sum_{\ell=1}^k \theta_{\ell} \quad \text{for } k = 0, 1, \dots, nm.$$

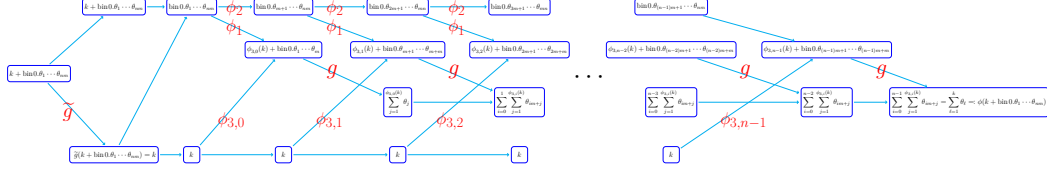


Figure 20: An illustration of the NestNet realizing ϕ based on Equations (16), (17), (18), (21), and (22). Here, g and \tilde{g} are regarded as activation functions.

1098 Note that $nm = n \cdot n^r = n^{r+1}$. Then we have

1099
$$\phi(k + \text{bin } 0.\theta_1 \dots \theta_{n^{r+1}}) = \sum_{\ell=1}^k \theta_\ell \quad \text{for } k = 0, 1, \dots, n^{r+1}.$$

1100 It remain to estimate the number of parameters in the NestNet realizing ϕ . Recall that ϕ_1 can
 1101 be realized by a one-hidden-layer \tilde{g} -activated network of width 1 and ϕ_2 can be realized by a
 1102 one-hidden-layer (σ, \tilde{g}) -activated network of width 2.

1103 Observe that

1104
$$\min\{a, b\} = \frac{1}{2}(\sigma(a+b) - \sigma(-a-b) - \sigma(a-b) - \sigma(-a+b)) \quad \text{for any } a, b \in \mathbb{R}.$$

1105 As we can see from Figure 21, $\phi_{3,i}$ can be realized by a σ -activated network of width 4 and depth 2
 1106 for each $i \in \{0, 1, \dots, n-1\}$.

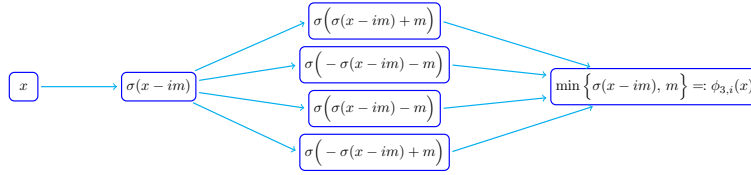


Figure 21: An illustration of $\phi_{3,i}$ for each $i \in \{0, 1, \dots, n-1\}$.

1107 Thus, the network in Figure 20 can be regarded as a (σ, g, \tilde{g}) -activated network of width $2 + 1 + 1 +$
 1108 $1 + 4 + 1 = 10$ and depth $2 + (2 + 1)n = 3n + 2$. Recall that $g \in \mathcal{NN}_r\{\widehat{n}\}$ and $\tilde{g} \in \mathcal{NN}_r\{72(r+7)n\}$.
 1109 This implies that ϕ can be realized by a height- $(r+1)$ NestNet with at most

1110
$$\underbrace{(10+1)10((3n+2)+1)}_{\text{outer network}} + \underbrace{\widehat{n}}_g + \underbrace{72(r+7)n}_{\tilde{g}} \leq \widehat{n} + 114(r+7)(n+1)$$

1111 parameters, which means we finish the proof of Lemma D.5.